



# Radio Frequency Technologies in Space Applications

Rosa Leon  
Jet Propulsion Laboratory  
Pasadena, California

Jet Propulsion Laboratory  
California Institute of Technology  
Pasadena, California

JPL Publication 10-11 10/10





# **Radio Frequency Technologies in Space Applications**

NASA Electronic Parts and Packaging (NEPP) Program  
Office of Safety and Mission Assurance

Rosa Leon  
Jet Propulsion Laboratory  
Pasadena, California

NASA WBS: 724297.40.49  
JPL Project Number: 103982  
Task Number: 03.02.13

Jet Propulsion Laboratory  
4800 Oak Grove Drive  
Pasadena, CA 91109

<http://nepp.nasa.gov>

This research was carried out at the Jet Propulsion Laboratory, California Institute of Technology, and was sponsored by the National Aeronautics and Space Administration Electronic Parts and Packaging (NEPP) Program.

Reference herein to any specific commercial product, process, or service by trade name, trademark, manufacturer, or otherwise, does not constitute or imply its endorsement by the United States Government or the Jet Propulsion Laboratory, California Institute of Technology.

Copyright 2010. California Institute of Technology. Government sponsorship acknowledged.

## **ACKNOWLEDGEMENTS**

Helpful discussions with Tien Nguyen, Charles Barnes, and Ken Label are gratefully acknowledged. The tables in the appendices showing available devices and vendors in radio frequency (RF) space technology are contributed from previous work by Jonathan Perret and James Skinner.

## TABLE OF CONTENTS

Abstract.....	1
1.0 Introduction .....	2
1.1 Background .....	2
1.2 RF Technology and Properties of III-V Materials .....	3
1.3 Heteroepitaxy of III-V Materials .....	5
1.4 Device Structures in RF Technology, Device Physics, and Materials .....	7
1.4.1 Bipolar Junction and Heterojunction Bipolar Transistors (BJTs and HBTs).....	7
1.4.2 Metal-Semiconductor Field-Effect Transistor (MESFET).....	9
1.4.3 High Electron Mobility Transistors (HEMTs).....	10
1.4.4 Metal Oxide Semiconductor Field Effect Transistor (MOSFETs).....	12
2.0 RF Devices Commonly Used in Space Applications .....	13
2.1 Low Noise Amplifiers (LNAs).....	13
2.2 Power Amplifiers (PAs) .....	14
2.3 RF Switches .....	16
2.4 Phase Modulators .....	17
2.5 Mixers and Multipliers .....	18
3.0 Measurements in RF Devices .....	20
3.1 Figures of Merit in RF Devices .....	20
3.1.1 Stability .....	20
3.1.2 S-Parameters .....	20
3.1.3 Power Gain.....	21
3.1.4 Characteristic Frequencies.....	22
3.1.5 Noise .....	23
3.1.6 Output Power and Power-Added Efficiency.....	23
3.1.7 Mean Time to Failure.....	24
4.0 Reliability Issues in RF Devices Used in Space Applications.....	25
4.1 General Reliability and Radiation Concerns.....	25
4.2 Hot Electron Effects .....	26
4.3 Radiation Tolerance of RF Devices.....	26
4.4 Quantifying Degradation in Life Tests .....	30
4.5 Modes of Failure in RF Devices .....	30
4.6 Electrostatic Discharge Failures.....	32
4.7 Electromigration .....	32
4.8 Other Failure Modes .....	33
4.9 Issues in Space RF Reliability.....	33
4.10 Space Qualification and Use of RF Devices—Recommendations .....	34
4.11 Studies Relevant to Space Use of RF Technology—Recommendations .....	35
5.0 References.....	37
Appendix A. Available Devices .....	39

## **ABSTRACT**

This body of knowledge (BOK) report on radio frequency (RF) device technology for space applications gives background on RF technology, device structures, device physics, fabrication processes, and materials used. A review of reliability concerns and known degradation/failure mechanisms are provided, and challenges in the space qualification of RF devices are identified. Previous JPL efforts in this area are included in the appendix, where available RF devices and vendors up to 2005 are listed.

## 1.0 INTRODUCTION

### 1.1 Background

Radio frequency (RF) devices are designed to operate at radio frequencies, defined as electromagnetic waves near and above 1 GHz (0.3 m). Older applications use lower frequencies as well, which are listed as high frequency (HF), very high frequency (VHF), and ultra high frequency (UHF) in Table 1.1-1, where as shown they span frequencies from 3 to 1 GHz. RF devices are also called microwave devices and they are used mostly as power amplifiers and transmitters in a variety of applications. Applications range from wireless communication, to jamming, radar, cell phones, imaging, DC/DC converters, and RF heating. Output powers from RF devices range from mili-Watts to mega-Watts; however, the small signal devices (low noise amplifiers) are by far more abundant and common than the RF power amplifiers.

**Table 1.1.1.** Bands available for fixed satellite services and other space applications of microwave radio frequencies.

RF Band	Frequency	Wavelength (meters)	Comments/Space Flight Use
HF	3–30 MHz	100–10	High frequency
VHF	30–300 MHz	10–1	Very high frequency
UHF	300–1000 MHz	1–0.3	Ultra high frequency
L	1–2 GHz	0.3–0.15	Long wave
S-	2–4 GHz	$1.5 \times 10^{-1}$ to $7.5 \times 10^{-2}$	Short wave. Used for communicating with piloted space missions
C- (G)	Earth-to-space frequencies 5.850–6.425 GHz Space-to-earth frequencies 3.6–4.2 GHz	$8.3 \times 10^{-2}$ to $4.8 \times 10^{-2}$	Compromise between S and X Satellite communication and spacecraft communications on Mercury and Gemini flights
X	8–12 GHz	$3.75 \times 10^{-2}$ to $2.5 \times 10^{-2}$	X for cross (as in crosshair) Used in WWII for fire control
Ku-	Earth-to-space frequencies 12.75–13.25, 13.75–14.8 GHz Space-to-earth frequencies 10.7–12.75, 17.3–17.7 GHz	$2.8 \times 10^{-2}$ to $1.7 \times 10^{-2}$	Kurz-under  Satellite communication
K	18–27 GHz	$1.6 \times 10^{-2}$ to $1.1 \times 10^{-2}$	Kurz (German for short)
Ka-	Earth-to-space frequencies 27.5–30.0 GHz Space-to-earth frequencies 17.7–21.2 GHz	$1.7 \times 10^{-2}$ to $9.9 \times 10^{-3}$	Satellite communication, satellite data relay services, interconnection of satellite, satellites in geostationary orbit (GSO) and over 500 in non-geostationary orbits
Q/V-	Earth-to-space frequencies 47.2–50.2 GHz Space-to-earth frequencies 39.5–42.5 GHz	$7.5 \times 10^{-3}$ to $5.9 \times 10^{-3}$	Satellite communication
E	71–6 GHz	$4.2 \times 10^{-3}$ to $3.5 \times 10^{-3}$	
W	Earth-to-space frequencies 80–110 GHz Space-to-earth frequencies 80–110 GHz	$3.73 \times 10^{-3}$ to $2.7 \times 10^{-3}$	W follows V in the alphabet
Sub millimeter	Earth-to-space frequencies 300 GHz–10 Terahertz Space-to-earth frequencies	$1 \times 10^{-3}$ to $3 \times 10^{-5}$ (1 mm – 30 micron wavelength)	Atmospheric sensing, radio astronomy, and infrared telescopes

In this report, the device physics, structures, and materials used in RF technology are discussed, as well as the figures of merit for different applications and the most common measurements relevant to RF technology. Quantifying degradation and modes of failure in RF devices are also addressed, as well as specific issues relating to space applications of RF technology.

RF is the frequency of electromagnetic radiation in the range at which radio signals are transmitted, ranging from approximately 3 kilohertz to 300 gigahertz. Many astronomical bodies, such as pulsars, quasars, and possibly black holes, emit radio frequency radiation. Table 1.1-1 lists the RF-band nomenclature associated with each frequency range used in most space applications, as well as the frequencies (and wavelengths of interest). Space applications are by no means the only use of RF devices: since the 1990s, cell phones created the first mass market for RF technology, with mobile internet access following shortly afterward. Another interesting connection between space applications and cellular phones pertains to the notable contributions of A. Viterbi, who worked in the area of “telecommunication spectrum technology” while working at JPL. His work included needed corrections for the Doppler effect for moving receivers and transmitters, which is important whether these are cell phones or spacecraft. He later invented the Viterbi algorithm, which he used for decoding convolutionally encoded data. It is still used widely in cellular phones for error correcting among many other applications.

RF devices are not always microwave-monolithic integrated circuits (MMICs); however, MMIC technology is needed to allow integration of complex microwave function like low-noise amplifiers (LNAs), front ends, receivers, frequency converters, and channel amplifiers. GaAs MMICs have the best performance, as well as reduced weight, reduced size, and reduced integration factor.

## 1.2 RF Technology and Properties of III-V Materials

RF technology uses materials like GaAs, Si, SiGe, InP, and even wide bandgap materials like SiC and GaP. III-V semiconductors can offer better high frequency performance. Gallium arsenide (and related compounds) are particularly useful in the high frequency/high data rate applications typically used for broadband and RF wireless components and of course, several types of satellite communications. The inherent physical properties of GaAs enable components based on this material to be as much as four to five times faster than their traditional silicon competitors. This is because the most important limitation on the transistors frequency response is the transit time of minority carriers across the base region, and this transit time is shorter as the electron mobility is increased. Some of the fundamental differences between device properties based on III-V semiconductors or group IV (Si and Ge) can be understood from the details of their band diagrams.

Figure 1.2-1 shows band diagrams comparing silicon, GaAs, and germanium [1] in some detail. These band diagrams show the energy plotted against the crystal momentum in two orthogonal crystal directions and can explain two very important features and differences between GaAs and group V semiconductors. One of them is the semiconductor’s ability to emit light, the other is the very high electron mobility found in GaAs and related compounds.

The bandgap is defined as the energy difference between the valence band maxima and the conduction band minima. In GaAs and other direct bandgap semiconductors, this energy gap is at the same point in the x axis at point  $\Gamma$ , whereas in Si and germanium, this minimum energy gap is near point X. Therefore, in Si and Ge, when an electron makes a transition from the valence

band to the conduction band, it requires not only energy change (equal or greater than the bandgap  $E_g$ ) but also a change in the crystal momentum. Since the likelihood of both transitions (enough change in energy and crystal momentum) is very low, only direct bandgap materials emit light when a carrier relaxes from the conduction band to the valence band. The energy of the photon emitted is that of the bandgap, and as will be shown later, the bandgap can be modified or “designed” with ternaries and quaternaries in the III-V family of compounds. While RF devices do not utilize the light emission capabilities of these devices, this property (emission of light equal in energy to the semiconductor bandgap) opens the possibilities for new types of device characterization based on their optoelectronic properties, which would not be suitable for Si devices.

Mobility is an important parameter for carrier transport, which in turn, limits device performance. Mobility describes how a carrier’s (hole or electron) motion is affected by an electric field.

The electron (or hole) drift velocity is:

$$v_d = \mu E$$

where  $v_d$  is the electron or hole drift velocity,  $E$  is the electric field and  $\mu$  is the mobility, either for the electrons or holes. The electron (or hole) mobility ( $\mu_{n(p)}$ ) is described as:

$$\mu_{n(p)} = q \frac{\tau}{m_{n(p)}}$$

Where  $q$  is the charge,  $\tau$  is the mean free time between collisions, and  $m_{n(p)}$  is the electron or hole effective mass. Qualitatively, it is easy to understand why the hole’s mobility is lower than the electron’s mobility: there is a lot more scattering in the valence band, hence, smaller mean time between collisions. As far as electron mobility, the curvature of the conduction band at the gamma point (at  $\Gamma$  shown in Figure 1.2-1) determines the electron effective mass. As can be seen from the band diagram of GaAs, such curvature is smaller in GaAs, resulting in a smaller electron effective mass, which explains the higher electron bulk mobility seen in Table 1.2-1. The very high mobilities arising from two dimensional electron gasses that are exploited in device applications are due to different phenomena, which will be covered in the section describing high-electron mobility transistors (HEMTs).

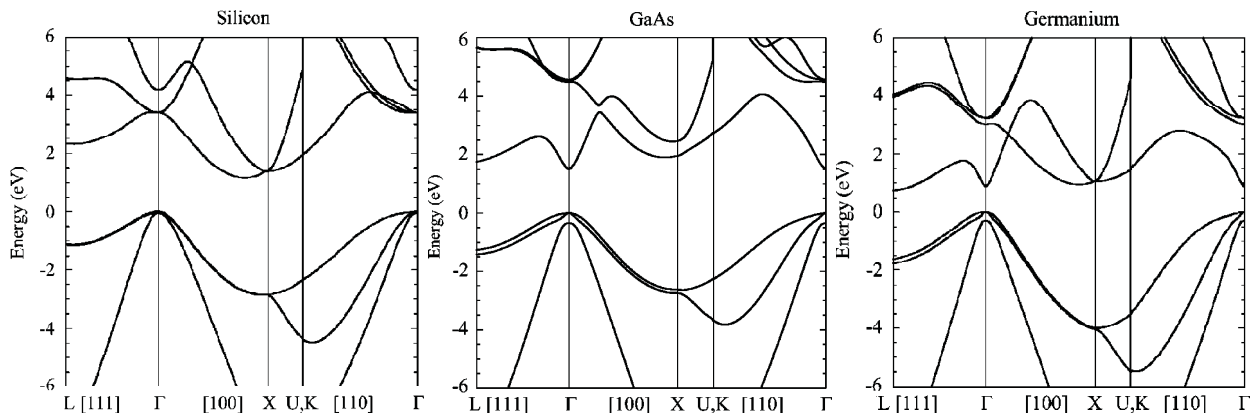


Figure 1.2-1. Band diagrams for common semiconductors comparing silicon, GaAs, and Ge.

**Table 1.2-1.** Comparison of properties of Si, Ge, and GaAs.

Properties	Si	Ge	GaAs
Atoms/cm <sup>3</sup>	5.0 x 10 <sup>22</sup>	4.42 x 10 <sup>22</sup>	4.42 x 10 <sup>22</sup>
Atomic Weight	28.09	72.60	144.63
Breakdown Field	Approx. 3 x 10 <sup>5</sup>	Approx. 1 x 10 <sup>5</sup>	Approx. 4 x 10 <sup>5</sup>
Crystal Structure	Diamond	Diamond	Zincblende
Density (g/cm <sup>3</sup> )	2.328	5.3267	5.32
Dielectric Constant	11.9	16.0	13.1
Effective Density of States in the Conduction Band, N <sub>c</sub> (cm <sup>-3</sup> )	2.8 x 10 <sup>19</sup>	1.04 x 10 <sup>19</sup>	4.7 x 10 <sup>17</sup>
Effective Density of States in the Valence Band, N <sub>v</sub> (cm <sup>-3</sup> )	1.04 x 10 <sup>19</sup>	6.0 x 10 <sup>18</sup>	7.0 x 10 <sup>18</sup>
Electron Affinity (V)	4.05	4.0	4.07
Energy Gap at 300 K (eV)	1.12	0.66	1.424
Intrinsic Carrier Concentration (cm <sup>-3</sup> )	1.45 x 10 <sup>10</sup>	2.4 x 10 <sup>13</sup>	1.79 x 10 <sup>6</sup>
Intrinsic Debye Length (microns)	24	0.68	2250
Intrinsic Resistivity (ohm-cm)	2.3 x 10 <sup>5</sup>	47	10 <sup>8</sup>
Lattice Constant (angstroms)	5.43095	5.64613	5.6533
Linear Coefficient of Thermal Expansion, ΔL/L/ΔT (1/°C)	2.6 x 10 <sup>-6</sup>	5.8 x 10 <sup>-6</sup>	6.86 x 10 <sup>-6</sup>
Melting Point (°C)	1415	937	1238
Minority Carrier Lifetime (s)	2.5 x 10 <sup>-3</sup>	Approx. 10 <sup>-3</sup>	Approx. 10 <sup>-8</sup>
Mobility (Drift) (cm <sup>2</sup> /V-s) μ <sub>n</sub> , electrons	1500	3900	8500
Mobility (Drift) (cm <sup>2</sup> /V-s) μ <sub>p</sub> , holes	475	1900	400
Optical Phonon Energy (eV)	0.063	0.037	0.035
Phonon Mean Free Path (angstroms)	76 (electron) 55 (hole)	105	58
Specific Heat (J/g-°C)	0.7	0.31	0.35
Thermal Conductivity at 300 K (W/cm-°C)	1.5	0.6	0.46
Thermal Diffusivity (cm <sup>2</sup> /sec)	0.9	0.36	0.24
Vapor Pressure (Pa)	1 at 1650°C; 10 <sup>-6</sup> at 900°C	1 at 1330°C; 10 <sup>-6</sup> at 760°C	100 at 1050°C; 1 at 900°C

Further advantages of GaAs and related III-V ternaries and quaternary compounds include better performance at both low and high temperatures, a higher activation energy for thermal interdiffusion, and an across-the-board better resistance to space radiation.

Also, because of its higher bandgap, and as seen in Table 1.2-1, pure GaAs is highly resistive. This allows isolation of different components that share one substrate, in this case, semi-insulating GaAs substrates.

### 1.3 Heteroepitaxy of III-V Materials

Some of the other important differences between the physical/chemical properties of III-V materials and silicon also have an effect on device performance, reliability, processing, and effective characterization techniques. However, the manufacture of III-V and some Si-Ge devices holds some complications that are not a concern in Si manufacturing. Some of these complexities can and often do have an effect on device reliability.

Some of these properties include thermal resistance, mechanical properties (more brittle), as well as optical properties; for example, Si is transparent at 4 microns, GaAs is not. Another crucial difference between Si and compound semiconductor devices lies not just in the individual differences between their properties that affect different aspects of device performance, but the way in which many compound semiconductors are manufactured. Figure 1.3-1 shows a diagram with the relationship between the lattice parameter in III-V materials and their corresponding bandgaps.

One of the important features in III-V devices is the built-in strain, which is unavoidable in the growth of strained interfaces. The active device areas are usually fabricated by epitaxial techniques, like molecular beam epitaxy (MBE) or metal organic chemical vapor deposition (MOCVD), which allow monolayer control when fabricating epitaxial structures. A diagram like the one shown in Figure 1.3-1 is used to determine what compositions will give the desired energy gaps, and how thick the epilayers of slightly mismatched materials can be grown without the introduction of dislocations. This thickness is usually referred to as the “critical thickness.” The composition of each atomic layer can be graded, for example, starting with GaAs and ending with InAs by making intermediate InGaAs of varying ternary compositions. Lattice mismatch engineering is a creative area in III-V semiconductor manufacture, which includes heteroepitaxy in Si substrates to increase mechanical strength and reduce costs. Lattice mismatch is accommodated by strain and this allows making InGaAs/InP devices for example. Some of the issues that arise with lattice mismatch are either curtailed or exploited in achieving performance that is only possible with compound epitaxial structures.

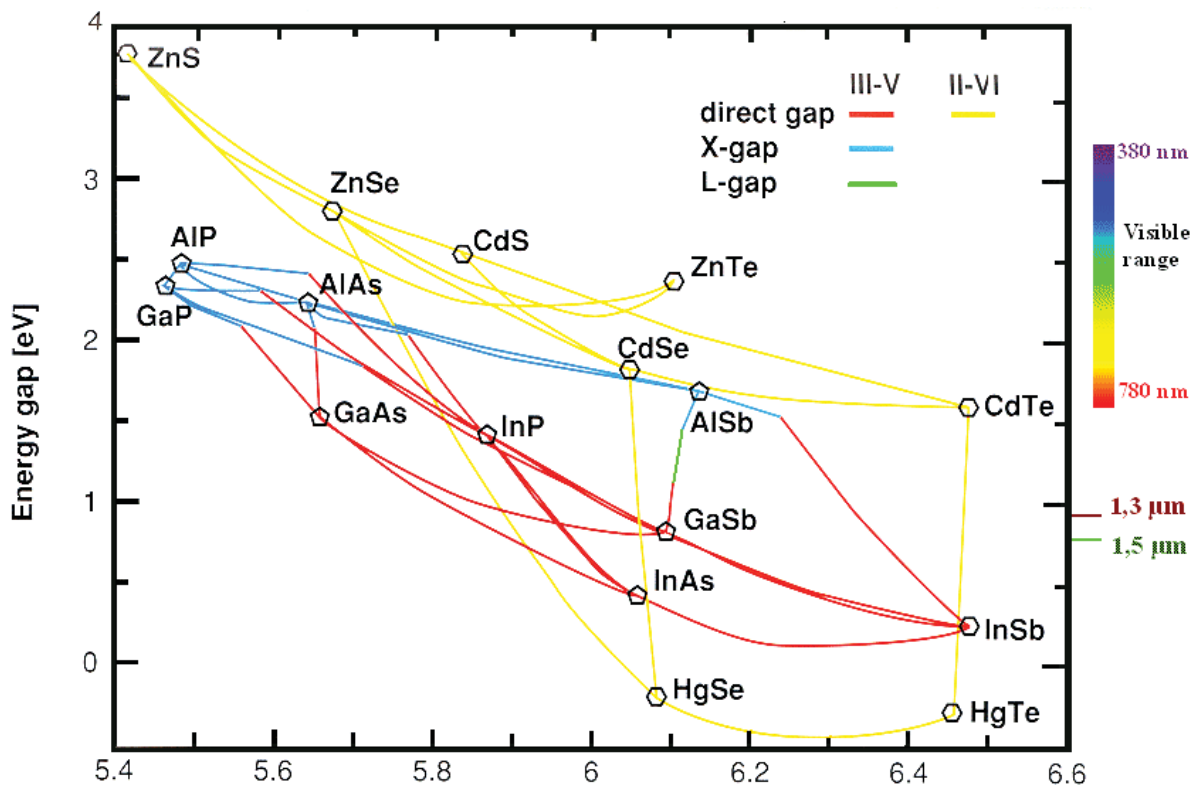


Figure 1.3-1. Energy gap (bandgap) for III-V and II-VI semiconductors as a function of lattice parameter (shown in Angstroms).

Some other differences with III-V materials include differences in oxide formation; AlGaAs, for example, must be protected from air and humidity or will oxidize. Different metals are used in forming ohmic contacts, Schottky barriers, and other metallization structures. These have many different properties regarding electromigration and oxidation as the metals used in silicon manufacturing. Passivating materials on GaAs devices are also different, and require different deposition technologies, etching, and processing.

Failure analysis of compound semiconductor devices also present special challenges. Etching rates, milling rates, and optical properties make sample preparation in failure analysis and electron microscopy of III-V devices different than silicon.

## **1.4 Device Structures in RF Technology, Device Physics, and Materials**

### ***Transistor Types by Configuration***

Among the different transistor configurations briefly covered here are bipolar junction transistors (BJT), heterojunction bipolar transistors (HBT), metal-semiconductor field-effect transistors (MESFET), high-electron mobility transistors (HEMT), pseudomorphic HEMT (pHEMT), metamorphic HEMT (mHEMT), and metal-oxide-semiconductor field-effect transistors (MOSFET).

In order to understand how these different devices are constructed and how they function, a brief mention needs to be made of doped semiconductors. Doping of semiconductors involves adding small amount of impurities found to the left or right column of the semiconductor being doped in the periodic table. These are called “shallow” impurities, since they form levels in the bandgap that are very close to the valence (acceptors) or conduction bands (donors). This is in contrast to “deep” levels, or impurities, that form much deeper levels. These can be acceptor or donor like, but are closer to the middle of the bandgap and act as electron-hole recombination centers, shortening both carrier lifetime and diffusion lengths. At room temperature, “shallow” impurities act as donors or acceptors, providing great control of the material’s resistivity (conductivity) and are designated either by n-type (dominated by donor impurities) or p-type (dominated by acceptor impurities).

#### **1.4.1 Bipolar Junction and Heterojunction Bipolar Transistors (BJTs and HBTs)**

BJTs are three-terminal electronic devices that make use of the properties of doped semiconductors for amplification and switching applications. They are known as “bipolar” because both electrons and holes are involved in their performance and operation. The main flow of electrons through them takes place in *two* types of semiconductor material, P and N, as the main current flows from emitter to collector (or vice versa). In other words, two types of charge carriers—electrons and holes—comprise the main current through the transistor. Charge travels across a junction between semiconductor regions of different doping concentrations. Most of the BJT collector current results from the flow of charged carriers injected from a region of high concentration (emitter) to a collector region, where such carriers are minority carriers (electrons in a p-type doped region or holes in an n-doped region). This is why BJTs are considered minority carrier devices. Bipolar transistors can be either PNP or NPN. The main current controlled goes from collector to emitter in the former, and from emitter to collector in the latter, as shown in Figure 1.4-1.

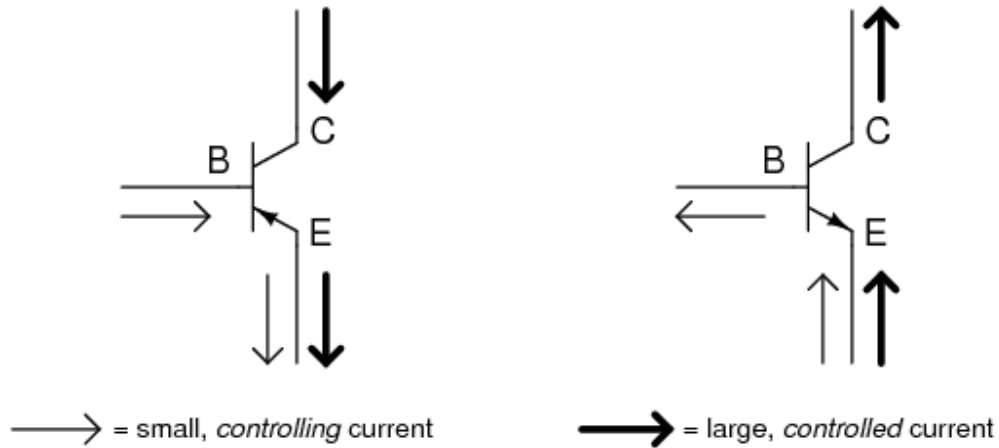


**Figure 1.4-1.** Types of bipolar transistors. The convention is to point the arrows against the direction of electron flow.

*Heterojunction Bipolar Transistor (HBT).* First proposed by H. Kroemer in 1957 [2], HBTs take advantage of the fact that using a wide bandgap emitter on a low bandgap base provides the needed band offset to favor electron injection into the base while retarding hole injection into the emitter. Figure 1.4-2 shows a band diagram and schematic structure of an HBT, respectively.

The main difference between the BJT and HBT is in the use of differing semiconductor materials for the emitter and base regions, creating a heterojunction. Injection of holes from the base to the emitter region is very limited due to the potential barrier in the valence band being higher than in the conduction band, once the two semiconductors form an interface. Unlike BJT technology, this allows a high doping density to be used in the base, reducing the base resistance while maintaining gain. HBTs can handle signals of very high frequencies up to several hundred GHz. They are common in modern ultrafast circuits, mostly RF systems (also known as microwave systems), as well as applications requiring a high power efficiency, such as power amplifiers in cellular phones.

Materials used for the substrate include silicon, gallium arsenide, and indium phosphide, while silicon/silicon-germanium, aluminum gallium arsenide/gallium arsenide, and indium phosphide/indium gallium arsenide are used for the epitaxial layers. Wide-bandgap semiconductors are especially promising, including gallium nitride and indium gallium nitride. In SiGe-graded heterostructure transistors, the amount of germanium in the base is graded, making the bandgap narrower at the collector than at the emitter. That tapering of the bandgap leads to a field-assisted transport in the base, which speeds transport through the base and increases frequency response.

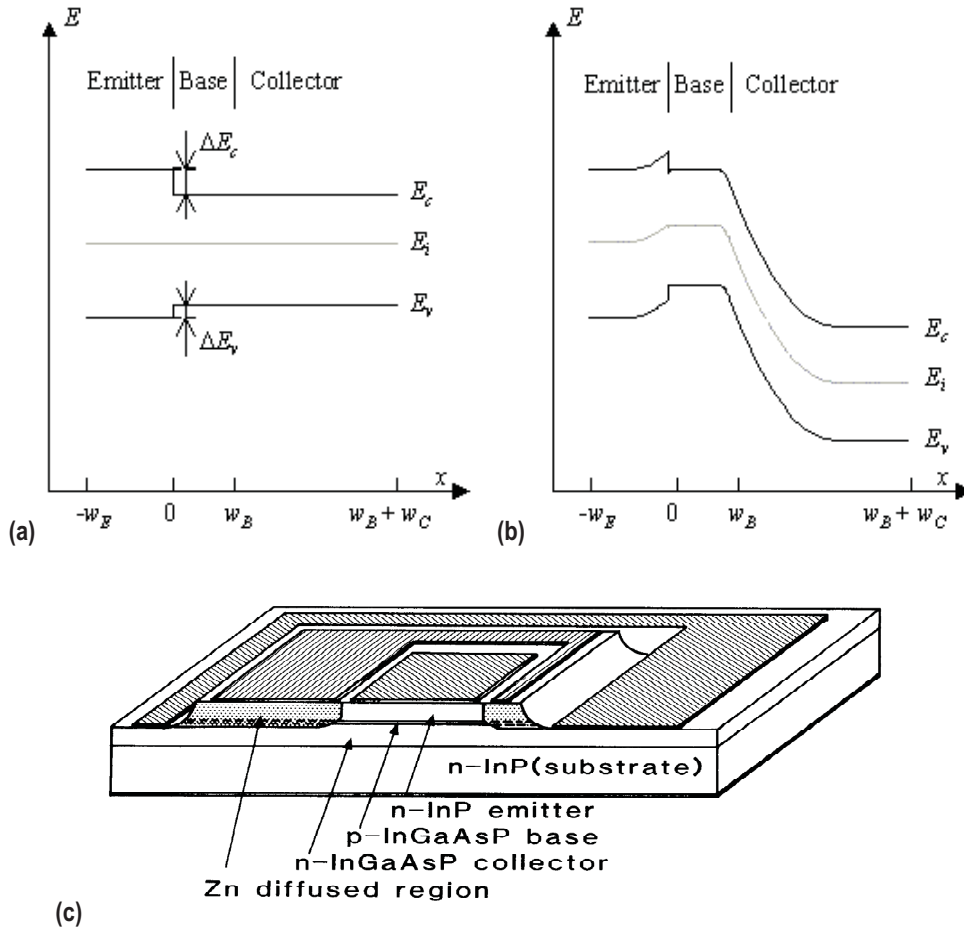


Figure 1.4-2. a) Flat-band energy band diagram, b) energy-band diagram under forward active bias, and c) Schematic structure of an InGaAsP/InP HBT [3].

### 1.4.2 Metal-Semiconductor Field-Effect Transistor (MESFET)

MESFETs have a conducting channel positioned between a source and drain contact region as shown in Figure 1.4-3. The carrier flow from source to drain is controlled by a metal gate known as a Schottky barrier. Control of channel current is obtained by varying the depletion layer width underneath the metal contact. This modulates the thickness of the conducting channel and thereby the current between source and drain.

The higher mobility of the carriers in the channel of MESFETs is one of their advantages as compared to MOSFETs. Carriers located in the inversion layer of a MOSFET have a wavefunction, which extends into the oxide; their mobility—also referred to as surface mobility—is less than half of the mobility of bulk material. As the depletion region separates the carriers from the surface, their mobility is close to that of bulk material. The higher mobility leads to a higher current, transconductance, and transit frequency of the device [4].

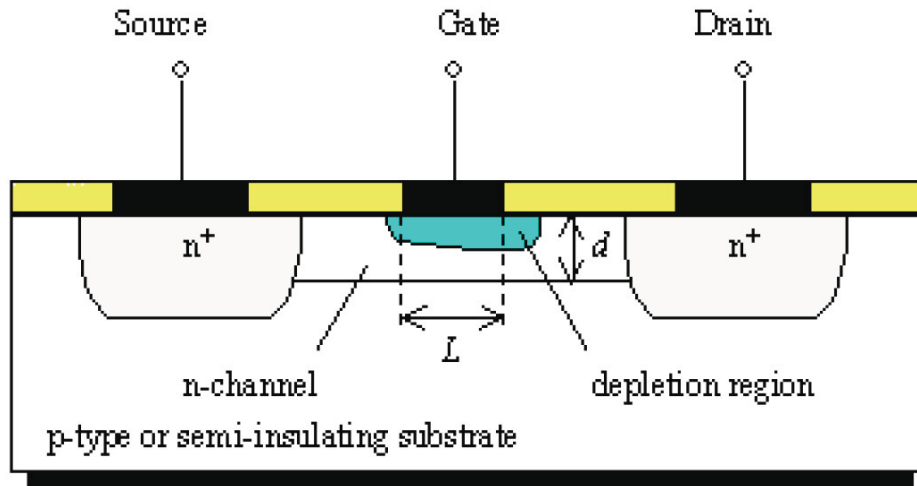


Figure 1.4-3. Structure of a MESFET with gate length  $L$ , and channel thickness  $d$ .

The main disadvantage of the MESFET structure is the Schottky metal gate, because it limits the forward bias voltage on the gate to the turn-on voltage of the Schottky diode. This turn-on voltage is typically 0.7 V for GaAs Schottky diodes. The threshold voltage therefore must be lower than this turn-on voltage. As a result it is more difficult to fabricate circuits containing a large number of enhancement-mode MESFET. The higher transit frequency of the MESFET makes it particularly interesting for microwave circuits. While the advantage of the MESFET provides a superior microwave amplifier or circuit, the limitation by the diode turn-on is easily tolerated. Typically, depletion-mode devices are used since they provide a larger current and larger transconductance and the circuits contain only a few transistors, so that threshold control is not a limiting factor. The buried channel also yields a better noise performance as trapping and release of carriers into and from surface states and defects is eliminated. The use of GaAs rather than silicon MESFETs provides two more significant advantages: first, the electron mobility at room temperature can be more than 5 times larger, while the peak electron velocity is approximately twice that of silicon. Second, it is possible to fabricate semi-insulating (SI) GaAs substrates, which eliminates the problem of absorbing microwave power in the substrate due to free carrier absorption.

### 1.4.3 High Electron Mobility Transistors (HEMTs)

HEMTs, also known as heterostructure FETs (HFETs) or modulation-doped FETs (MODFETs) are FETs that include a junction between two dissimilar materials, or material with a different bandgap. Such junction is called a heterojunction, which acts as the channel, in contrast to the doped region used in MOSFET devices. GaAs/AlGaAs is the most common materials combination for HEMTs, even though other combinations are also used, depending on the expected application. Devices that incorporate indium (as InGaAs or InGaP) show good high frequency performance, and GaN-based HEMTs are of great interest as well, due to their high-power performance and high-temperature robustness.

HEMTs are devices based on the physics of a *two-dimensional electron gas* (2DEG). A 2DEG is a gas of electrons free to move in two dimensions, but tightly confined in the third. This tight confinement leads to quantized energy levels for motion in the confinement direction, but these are not typically used in the device performance. The electrons therefore appear to be a two-

dimensional (2D) sheet embedded in a 3D world. A diagrammatic drawing of such a structure is shown in Figure 1.4-4. An equivalent structure based on holes rather than electrons is called a two-dimensional hole gas (2DHG), and such systems have many useful and interesting properties based on the physics of a 2D electron gas. It is possible to confine electrons (or holes) in a 2D layer (a 2D electron gas, called a 2DEG, or, for holes, a 2DHG) in a crystal, in such a way that they can move within that layer with minimal scattering. Such systems show quantum-mechanical properties such as the integer and the fractional quantum Hall effects [5]. Patterned gates above and below the 2DEG can be used to further confine the electrons into narrow one, and zero-dimensional regions.

In order to form a conducting region with mobile electrons, a portion of the semiconductor material is normally doped with n-type impurities. At room temperature, the extra electrons from these impurities are ionized, and the electrons are free to move. However, their mobility is diminished due to collisions that occur with the doping impurities or other impurities.

Using the band offsets shown in Figure 1.4-4, a 2D electron gas can be formed. In this case, the electrons alone (without any associated dopant impurity atoms) are formed in the thin AlGaAs layer and “trapped” or “confined” right below the AlGaAs layer, in the GaAs adjacent to it, by the potential barriers involved, which effectively form a quantum well. This adjacent GaAs layer is undoped, so it contains no added impurities. Since these are electrons with 2D freedom of motion—known as a 2D electron gas—that have no scattering centers to slow them down, extremely high-electron mobilities can be achieved. This concept of 2-deg (2D electron gas) is the whole idea behind the operation of HEMTs. As with all the other types of FETs, a voltage applied to the gate alters the conductivity of this layer.

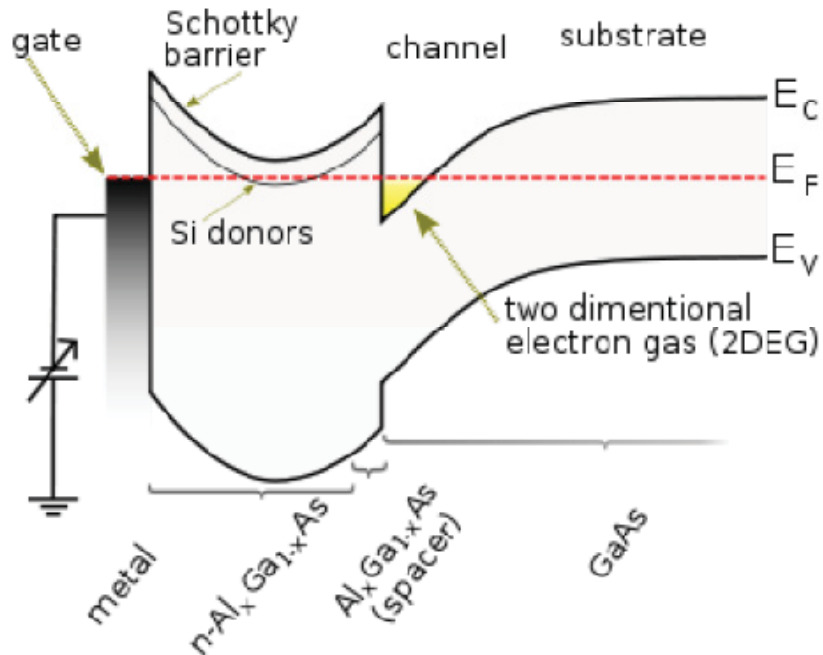


Figure 1.4-4. Band structure in GaAs/AlGaAs heterojunction-based HEMT.

A quick glance at Figure 1.3-1 should convince the reader that AlGaAs and GaAs are “lattice matched,” meaning that they have almost the same lattice constant. Lattice-matched materials can be grown epitaxially without dislocations or other interface defects, even though anti-phase boundaries can still be present if the materials have different crystal structures (like GaAs and Ge or Si for example). This makes it very convenient to form heterojunctions in between these two materials, so one can obtain a confining potential with a structure that maintains the same lattice constant and can be grown defect-free. This is one reason why the AlGaAs/GaAs material combination is so popular.

While the same lattice constant is necessary for successful growth of thick layers, it is possible to grow just a few mono-atomic layers of a crystalline material on another that has a different lattice parameter (but it should still be the same basic crystal structure). Some HEMTs that violate the guideline of matching crystal lattices in epitaxy are called pHEMTs, or pseudomorphic HEMTs. This is achieved by using an extremely thin layer of one of the materials—so thin that the crystal lattice simply stretches to fit the other material, but accumulates a lot of residual strain. This technique allows the construction of transistors with larger bandgap differences than otherwise possible, giving them the potential for better performance.

Another way to use materials of different lattice constants is to place a buffer layer between them. This is done in the mHEMT, or metamorphic HEMT, an improvement on the pHEMT. The buffer layer is made of InAlAs, where the indium concentration is adjusted gradually or graded, so that it can match the lattice constant of both the GaAs substrate and the InGaAs channel. This strategy allows optimization for different applications (low indium concentration provides low noise; high-indium concentration gives high gain).

Applications for HEMTs are similar to those of MESFETs: microwave- and millimeter-wave communications, radar, imaging, and radio astronomy. These are applications that require high gain and low noise at high frequencies. HEMTs have shown current gain at 600 GHz and power gain at 1 THz. HEMTs are manufactured worldwide and are more commonly used in monolithic-microwave integrated circuits or MMICs.

#### **1.4.4 Metal Oxide Semiconductor Field Effect Transistor (MOSFETs)**

The **MOSFET** type of field effect transistor has a “metal oxide” gate (usually silicon dioxide commonly known as glass), which is electrically insulated from the main semiconductor N-channel or P-channel. This isolation of the controlling gate makes the input resistance of the **MOSFET** extremely high in the Mega-ohms region. As the gate terminal is isolated from the main current carrying channel, no current flows into the gate, and like the junction-gate field effect transistor (JFET) the **MOSFET** also acts like a voltage-controlled resistor. Also like the JFET, this very high input resistance can easily accumulate large static charges resulting in the **MOSFET** becoming easily damaged unless carefully handled or protected.

## 2.0 RF DEVICES COMMONLY USED IN SPACE APPLICATIONS

Among the most common RF devices used in space hardware are LNAs, power amplifiers, RF switches, phase modulators, and mixers/multipliers. A brief background on applications, device operation, materials, and device configurations is provided below.

### 2.1 Low Noise Amplifiers (LNAs)

LNAs are key components in millimeter-wave radar and radiometer system applications. They are widely used in wireless communications, and can be found in almost all RF and microwave commercial applications such as cordless telephones, cellular phones, wireless local area networks, satellite uplinks/downlinks, and in military applications such as Doppler radars and signal interceptors. G-band LNAs (known also as C-band in the older nomenclature) are of importance in space applications, and are used in weather forecasting and tracking of storms.

The purpose of an LNA is to boost the desired signal power while adding as little noise and distortion as possible so that retrieval of this signal is possible in the later stages in the system. With this in mind, LNA designers have developed many design concepts and theories applied to LNAs and important figures of merit used to characterize and compare their performance. Figures of merit are as high a gain as possible (usually given in dB) and as low a figure for noise as possible (also given in dB at a given frequency or frequency range of interest). Since LNAs are used to amplify weak signals, they are usually placed very close to the detection devices in order to reduce losses due to coaxial cable lines. They are placed at the front end of a radio receiver circuit, immediately following the antenna. Since any noise from the LNA will be injected directly into the received signal, LNAs should amplify the desired signals while adding as little noise and distortion as possible.

Since the amplifiers need to have high amplification in their first stage, JFETs and HEMTs are considered good choices for LNAs. Devices used as LNAs include Si and SiGe BJTs, GaAs FETs, GaAs MESFETs, GaAs pHEMTs, GaAs HBTs, and SiGe HBTs. Table A-1 in Appendix A [6] lists examples of available devices.

In LNAs, noise reduction and gain enhancement take priority over energy/power efficiency, primarily in military/space applications, so large biasing resistors are used to prevent weak signal leakage, and the HEMTs are driven in the high-current regime, which reduces the relative amount of shot noise. Input and output matching circuits are also used in narrow band circuits to increase the gain. A band pass filter may be required in front of it if there are many adjacent interfering bands leaking through the antenna, but this filter generally degrades the noise performance of the system.

Area of research and technology development is extending the range of the LNA to the submillimeter and Terahertz regions. GaAs MMICs are developed in the 29–36 GHz (Ka and/or E bands). Over the past two decades, the military market has widely embraced the use of MMICs. The MMIC Program of the mid-1980s brought about significant advances in the design, manufacture and test capability of GaAs MMIC components. The advantages of using MMICs over their MIC/discrete hybrid counterparts include lower total cost, easier assembly, and more consistent performance. The impact and magnitude of these advantages increases with the frequency of operation. Components used in today's military systems must exhibit very high performance, and be robust enough to operate in harsh land-, sea- and air-based environments. MMICs achieve the most consistent results at Ka-band.

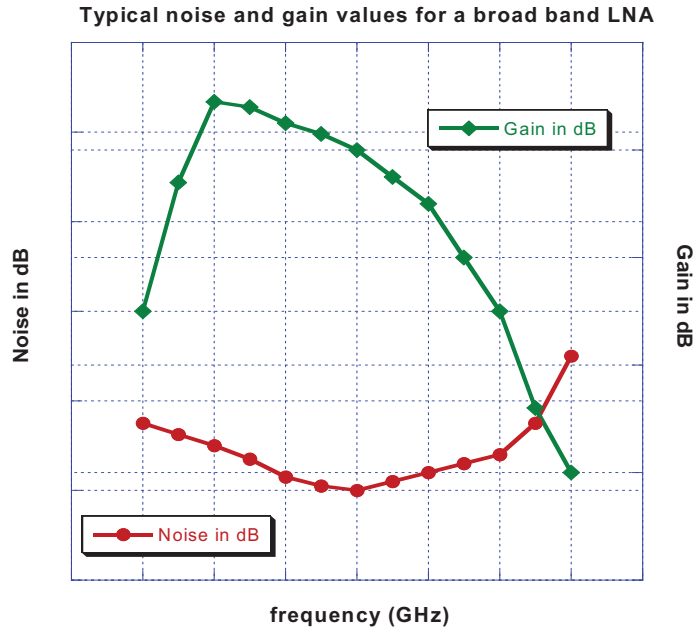


**Figure 2.1-1.** Typical specification curve for an LNA, showing noise and gain as a function of frequency.

GaAs LNA MMICs are available from different vendors. Usually specifications show gain and noise figures as a function of frequency (see Figure 2.1-1 for an example).

While these devices are used across the whole frequency spectrum, they are most frequently used in intermediate frequencies, the Ka-band; in particular, the 29 to 36 GHz band is the focus of many important applications of MMIC LNA components.

RF absorption of the atmosphere is negligible around the middle of this band (29–36 GHz), which is the main reason for so many military applications as well as satellite communications using it. For military applications, another specification to give attention to is the noise and gain values at the thermal extremes. Low, small, or no variation in gain and noise avoids overdesigning the linearity of the RF chain, potentially driving up DC power consumption, in order to meet system-level specifications at the operating temperature extremes.

## 2.2 Power Amplifiers (PAs)

RF power amplifiers (PAs) are used in a multitude of applications in space, for satellites, radios, radars, telemetry, and communication systems. A solid-state power amplifier is a circuit for electronic amplifiers that is used to convert low-power radio frequency signals or DC input power into a significant amount of RF/microwave power, typically used for driving the antenna of a transmitter. Power amplifiers are usually optimized to have high efficiency, high power compression, good return loss on the input and output, good gain, and optimum heat dissipation. There are a great variety of power amplifiers, and they have been significantly improved in recent years. The major advantages of such amplifiers for space applications are their high reliability, low mass and small dimensions, high degree of linearity, and improved system flexibility. In this context, high-power microwave field-effect transistors (FETs) with internal matching have recently appeared on the market as devices which are very compact, very reliable, and capable of handling sufficient RF power to be suitable for use on board of space vehicles.

In communications applications, most power amplifiers are operated at high frequency. For example, the RF power amplifiers used in mobile phones typically operate at a frequency of several gigahertz (GHz). For space-based communications, the amplifier may operate at frequencies of tens of gigahertz. This very high frequency range means that the traditional complementary metal-oxide semiconductor (CMOS) process cannot be used to manufacture the amplifier economically. Therefore, different high-mobility semiconductor materials are commonly used, such as GaAs, SiGe, or other III-V group semiconductor materials. The most commonly used building blocks of these amplifiers are not CMOS transistors; rather, types such as MESFETs, HBTs, pHEMTs, and lateral-diffused metal-oxide-semiconductor transistors (LDMOSs) that were discussed in the previous section are often used. This is reflected in the devices available from today's vendors seen in Table A-2 in Appendix A [6].

Figure 2.2-1 shows the MESSENGER solid-state power amplifier, an example of space use of power amplifiers. The lumped amplifier section feeds a 40-dBm RF signal to the fan beam and LGAs. The RF power divider board splits the RF signal to feed the various stick amplifiers in the distributed amplifier sections, which in turn feed RF power to the phased-array antennas. The digital board serves as the command and telemetry interface to the spacecraft. A 6-in (15.2-cm) ruler in the photograph indicates scale [7].

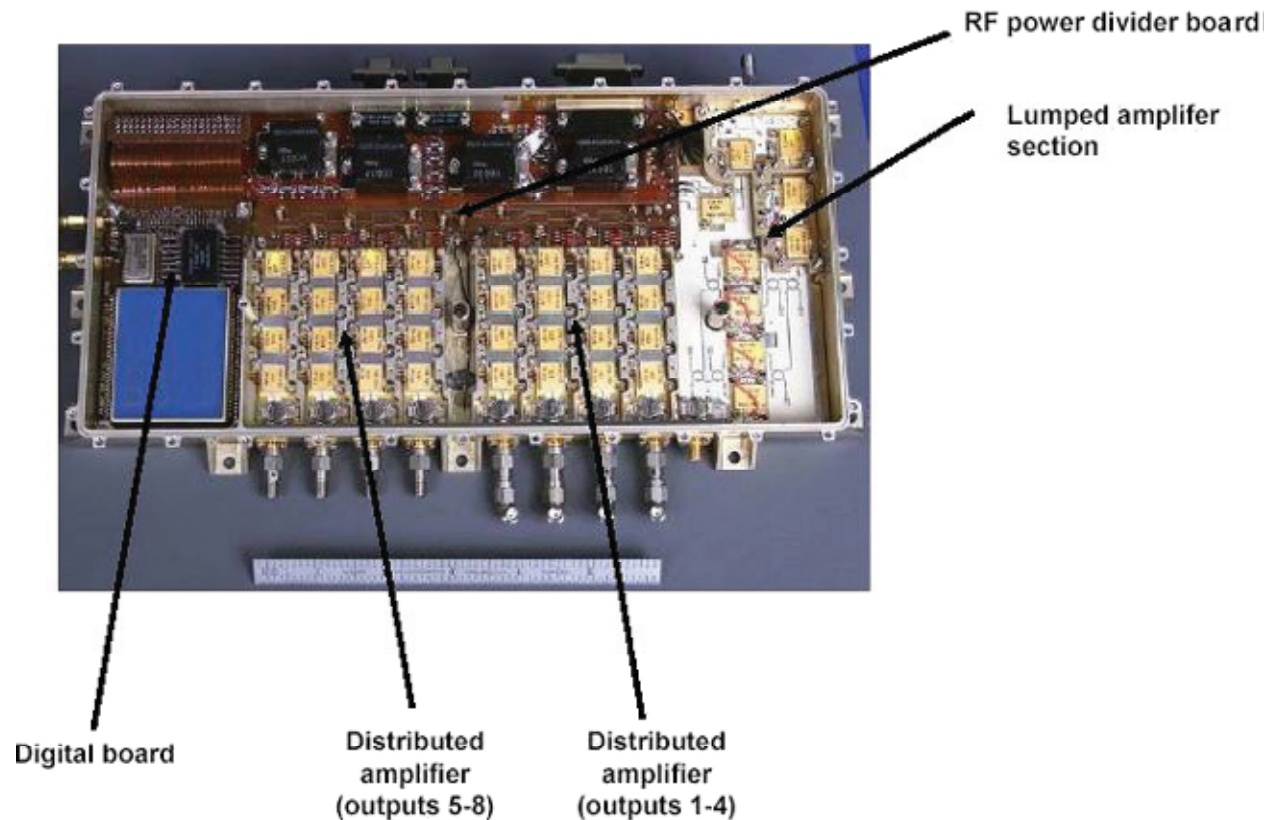


**Figure 2.2-1.** The MESSENGER solid-state power amplifier, an example of space use of power amplifiers. A 6-in (15.2-cm) ruler indicates scale [7].

Modern wireless communication base stations transmit and receive RF signals through the use of RF power amplifiers. An RF signal may be transmitted through air, free space, coaxial cable, fiber optic cable, etc. An RF transmitter mixes the desired signal, known as the baseband signal, with an RF carrier frequency for transmission over the selected medium. An RF receiver then mixes the signal with the carrier frequency to restore the signal to its original frequency. RF transmission typically occurs at a single band for specific applications such as cellular phone transmissions. Typical cellular phone transmission bands include 800 MHz and 1,900 MHz in the United States, and 900 MHz and 1,800 MHz in most countries in Europe and Asia. Radio frequency devices transmit an information signal from one point to another by moving the information signal to a higher frequency range that is more suitable for transmission over the medium being used. This process is known as up conversion. In operation, a power amplifier circuit receives an RF signal in the transmit path of the communication device, amplifies the RF signal, and provides the amplified signal to an antenna. To meet system requirements, the RF antenna power output must be maintained substantially constant.

Other applications include testing requirements where a relatively large amount of RF power is necessary for overcoming system losses to a radiating element, such as may be found at a compact range, or where there is a system requirement to radiate a device-under-test (DUT) with an intense electromagnetic field, as may be found in EMI/EMC applications.

As varied as the system requirements may be, the specific requirements of a given amplifier can also vary considerably. Nevertheless, there are common requirements for nearly all amplifiers, including frequency range, gain/gain flatness, power output, linearity, noise figure/noise power, matching, and stability. Often there are design trade-offs required to optimize any one parameter over another, and performance compromises are usually necessary for an amplifier that may be used in a general purpose testing application.

### **2.3 RF Switches**

RF switches are most often used to connect an antenna alternately to a transmitter and receiver. Most RF switches are based on GaAs technology. GaAs-based FETs consume very little DC power, and offer a good “on” to “off” impedance ratio, which translates into low insertion losses and good isolation.

RF switches, also called multiplexers, can also be based on CMOS technology. High-bandwidth CMOS switches and multiplexers are available. When designing an RF switch network, the following must be considered: characteristic impedance, bandwidth, topology, insertion losses, return loss and voltage standing-wave ratio (VSWR), isolation/crosstalk, and rise time.

At high frequency (or short wavelengths), the values inside a cable will vary (in a sinusoidal wave) and there will be reflection losses. This is why at high frequency, different materials and configurations are needed, to minimize reflection losses due to the dimensions of the wave being much smaller than the cable length. This is where different impedances mediums and characteristic impedance of a transmission line are important. Impedance matching is done in order to minimize signal losses reflections; the properties of the materials in the transmission line are important since impedances must be matched there too. Insertion losses start to be substantial causing power loss and voltage attenuations when the length of the transmission line is over 10% of its wavelength frequency.



**Figure 2.3-1.** MEMS RF switches with metallic waveguides and conventional RF switches. Full mechanical switches provide high reliability for wireless terminal testing up to 5GHz.

The number of throws in the intended RF switch application is important, as well as the switch topology. Handling both transmitter and receiver power levels increases the complexity of the switch design, since the RF signal must be transmitted without distortion or creating harmonics. Table A-3 in Appendix A [6] lists examples of available RF switch devices. Figure 2.3-1 shows pictures of different types of RF switches available today.

Micro-electro-mechanical systems (MEMS) RF switches are also becoming available as a commercial option. These are miniaturized mechanical devices for switching high-frequency electromagnetic signals. The advantages of MEMS RF switches compared to p-type-intrinsic-n-type (PIN) diodes and FETs are minimum insertion loss, maximum isolation, superior signal linearity, and very low power consumption.

Another very important consideration in RF switch applications is the amount of RF power that must be allowed to pass (or prevent from passing). The power handling of the RF switches is specified by different parameters, but a very common one is the 1 dB compression point. This is defined as either the input or output power at which the insertion loss increases by 1 dB from its small signal value. Insertion losses are frequency dependent. Here are some expressions for calculating power losses and voltage attenuation in RF switches:

For calculating power loss:

$$\text{Insertion loss (dB)} = 10\log_{10}(P_{\text{out}}/P_{\text{in}})$$

For calculating voltage attenuation:

$$\text{Insertion loss (dB)} = 20\log_{10}(V_{\text{out}}/V_{\text{in}})$$

## 2.4 Phase Modulators

Phase modulation (PM) is a method of impressing data onto an alternating-current (AC) waveform by varying the instantaneous phase of the wave. This scheme can be used with analog or digital data.

In analog PM, the phase of the AC signal wave, also called the *carrier*, varies in a continuous manner. Thus, there are infinitely many possible carrier phase states. When the instantaneous data input waveform has positive polarity, the carrier phase shifts in one direction; when the instantaneous data input waveform has negative polarity, the carrier phase shifts in the opposite direction. At every instant in time, the extent of carrier-phase shift (the *phase angle*) is directly proportional to the extent to which the signal amplitude is positive or negative.

In digital PM, the carrier phase shifts abruptly, rather than continuously back and forth. The number of possible carrier phase states is usually a power of 2. If there are only two possible phase states, the mode is called *biphase modulation*. In more complex modes, there can be four, eight, or more different phase states. Each phase angle (that is, each shift from one phase state to another) represents a specific digital input data state.

Phase modulation is similar in practice to frequency modulation (FM). When the instantaneous phase of a carrier is varied, the instantaneous frequency changes as well. The converse also holds: When the instantaneous frequency is varied, the instantaneous phase changes. But PM and FM are not exactly equivalent, especially in analog applications. When an FM receiver is used to demodulate a PM signal, or when an FM signal is intercepted by a receiver designed for PM, the audio is distorted. This is because the relationship between phase and frequency variations is not linear; that is, phase and frequency do not vary in direct proportion.

Table A-4 in the Appendix shows some PM devices commercially available today.

## 2.5 Mixers and Multipliers

GaAs varactor multipliers and GaAs mixer diodes for submillimeter and THz receivers used in radio astronomy are targeted for very diverse applications. These range from the detection of naturally occurring microwave thermal emission from the limb of Earth's atmosphere in NASA's Micro Limb Sounder (MLS) instrument, to the joint NASA/ESA FIRST mission infrared-submillimeter detection of the dusty galaxies from which no visible light can escape (the major extragalactic sources in this wavelength interval). Despite this apparent divergence in scientific research goals, GaAs-based RF devices of almost identical structure are common reliability concerns in both these missions, and in several other future and planned applications of submillimeter-wave radio astronomy.

While the present state of technology can accommodate frequencies up to Q-band, and possibly up to W-band with commercially available devices, submillimeter-wave frequencies can be obtained only from devices still in research and development stage. Despite the unknowns in the reliability of these research devices, these are already being used in space flight, and are essential components of several Earth Observing System (EOS) MLS and also in various orbiting infrared space telescopes, like Herschel and Planck.

There are numerous millimeter- and submillimeter-wave space applications that require power sources for transmitters, and low-noise local oscillators for receivers and arrays. At the highest frequencies, GaAs-based, solid-state frequency multipliers are used to efficiently transfer the output of lower frequency sources to harmonic frequencies. Nonlinearities in either the I-V or the C-V characteristics of these devices offer the possibility of frequency multiplication. It is well known that the power handling capability of familiar low frequency solid-state devices is relatively low, especially at higher frequencies (i.e., >100 GHz). At frequencies exceeding 250 GHz, GaAs-based varactor multipliers offer the highest solid-state power output, making them promising candidates as reference local oscillator (LO) sources. Schottky diode mixers are also showing very promising characteristics and remain the element of choice as receivers for the shortest submillimeter wavelengths. A mixer is any device used to multiply signals that have a nonlinear response to an electric field. Mixers combine a RF signal and an LO. The result of the multiplication for two co-sinusoidal signals is then applied to a filter that only accepts the bandwidth of interest. Figure 2.5-1 shows an example of a CMOS low-noise mixer [8].

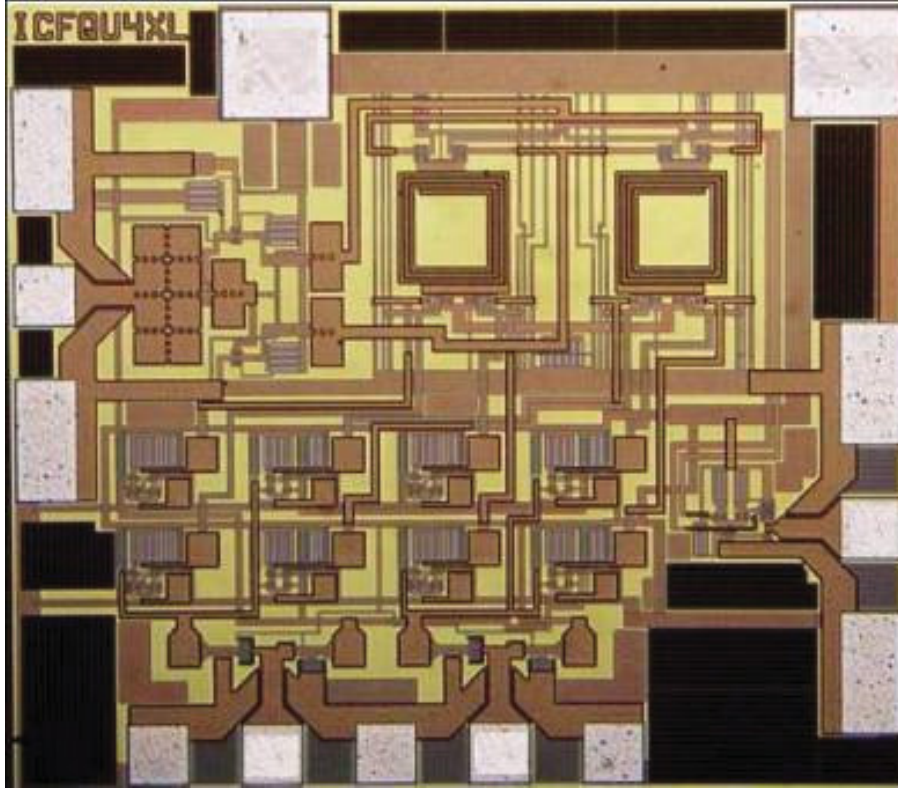


Figure 2.5-1. Low-noise mixer based on CMOS technology [8].

## 3.0 MEASUREMENTS IN RF DEVICES

RF devices are often evaluated using the concept of “figures of merit.” A figure of merit is simply a meaningful measurement to make, so that engineers can quantify and estimate device performance, as well as compare performances for different RF devices within the same class.

The most often used figures of merit are stability, power gain, characteristic frequency, noise, output power, power added efficiency, and mean time to failure (MTTF) [9].

Some of the measurement techniques, including some advanced techniques, involve pulsed IV measurements, load-pull measurements, probing, sampling, and sensing techniques. Recent advances in measurements using vector network analyzers have also been incorporated into RF devices and are used to measure non-linear performance of these devices [10].

### 3.1 Figures of Merit in RF Devices

#### 3.1.1 Stability

Stability, in referring to amplifiers, refers to an amplifier’s immunity to causing spurious oscillations. The oscillations can be full-power, large-signal problems, or more subtle spectral problems that might not be noticed unless the output is carefully examined with a spectrum analyzer. Unwanted signals may be nowhere near the intended frequency but will wreak havoc all the same. This type of problem is to be avoided. Stability can be either conditional or unconditional.

**Conditional stability** refers to a network that is stable when its input and output “see” the intended characteristic impedance  $Z_0$  (usually 50 ohms, sometimes 75 ohms), but if the application presents a mismatch, there is a region of either source or load impedances that will definitely cause it to oscillate.

**Unconditional stability** refers to a network that can “see” any possible impedance on the Smith chart from the center to the perimeter (up to  $\gamma = 1.0$ ) at any phase angle.  $\gamma < 1$  means that the real part of the impedance is positive. Note that any network can oscillate if it sees a real impedance that is negative; therefore, if a system goes outside the normal Smith chart, chances of stability are slim.

Stability has to be separately evaluated at all frequencies where the amplifier could potentially oscillate. This is generally up to the maximum frequency  $f_{\max}$  of the technology. For power pHEMT parts, stability is not a problem past around 50 GHz.

#### 3.1.2 S-Parameters

S-parameters refer to the scattering matrix (“S” in *S-parameters* refers to *scattering*). The concept was first popularized around the time that Kaneyuke Kurokawa of Bell Labs wrote his 1965 IEEE article *Power Waves and the Scattering Matrix* [11].

The scattering matrix is a mathematical construct that quantifies how RF energy propagates through a multi-port network. The S-matrix is what allows us to accurately describe the properties of incredibly complicated networks as simple “black boxes.” For an RF signal incident on one port, some fraction of the signal bounces back out of that port, some of it *scatters* and exits other ports (and is perhaps even amplified), and some of it disappears as heat or even

electromagnetic radiation. The S-matrix for an N-port contains  $N^2$  coefficients (S-parameters), each one representing a possible input-output path.

S-parameters are complex (magnitude and angle) because both the magnitude and phase of the input signal are changed by the network. However, S-parameters are usually described by magnitude only, as it is of the most interest, since the magnitude of gain or loss is the most important. S-parameters are defined for a given frequency and system impedance, and vary as a function of frequency for any non-ideal network.

S-parameters refer to RF “voltage-out versus voltage-in” in the most basic sense. S-parameters come in a matrix, with the number of rows and columns equal to the number of ports. For the S-parameter subscripts “ij,” j is the port that is excited (the input port), and “i” is the output port. Thus,  $S_{11}$  refers to the ratio of signal that reflects from port one for a signal incident on port one. Parameters along the diagonal of the S-matrix are referred to as reflection coefficients because they only refer to what happens at a single port, while off-diagonal S-parameters are referred to as transmission coefficients, because they refer to what happens from one port to another. The following are the S-matrices for one-, two- and three-port networks:

$$\begin{aligned}
 & [S_{11}] \text{ (one port)} \\
 & \begin{bmatrix} S_{11} & S_{12} \\ S_{21} & S_{22} \end{bmatrix} \text{ (two port)} \\
 & \begin{bmatrix} S_{11} & S_{12} & S_{13} \\ S_{21} & S_{22} & S_{23} \\ S_{31} & S_{32} & S_{33} \end{bmatrix} \text{ (three port)}
 \end{aligned}$$

Note that each S-parameter is a vector, so if actual data were presented in matrix format, a magnitude and phase angle would be presented for each  $S_{ij}$ .

S-parameter magnitudes are presented in one of two ways, linear magnitude or decibels (dB). Because S-parameters are a voltage ratio, the formula for decibels in this case is

$$S_{ij}(\text{dB}) = 20 * \log[S_{ij}(\text{magnitude})]$$

The angle of a vector S-parameter is almost always presented in degrees (but of course, radians are possible).

When we are talking about networks that can be described with S-parameters, we are usually talking about single-frequency networks. Receivers and mixers are not referred to as having S-parameters, although you can certainly measure the reflection coefficients at each port and refer to these parameters as S-parameters. The trouble comes when you wish to describe the frequency-conversion properties; this is not possible using S-parameters.

### 3.1.3 Power Gain

Gain can be defined as the ability to amplify currents and voltages. This is also defined as the ratio of power supplied from the transistor output to the load, over the power delivered to the transistor input from the signal source.

Power gains are given in decibels. If we take P2 as the delivered transistor output, and P1 as the power at transistor input:

$$P2/P1[\text{dB}] = 10 \log (P2/P1)$$

The transfer of power is dependent on impedance matching conditions. Maximum available gain can only happen when power matching happens. To achieve power matching, the input and output of the transistor need to be conjugately impedance-matched to the signal source and the load, respectively. This would give the maximum available gain (MAG) for the transistor.

Three important types of power gains are operating power gain, transducer power gain, and available power gain.

### **Operating Power Gain**

The operating power gain of a two-port network  $G_P$  is defined as:

$$G_P = \frac{P_{load}}{P_{input}}$$

where

$P_{load}$  is the average power delivered to the load

$P_{input}$  is the average power entering the network

This is the power gain at the amplifier's operating frequency.

### **Transducer Power Gain**

The transducer power gain of a two-port network,  $G_T$ , is defined as:

$$G_T = \frac{P_{load}}{P_{source,max}}$$

where

$P_{load}$  is the average power delivered to the load

$P_{source,max}$  is the maximum available average power at the source

### **Available Power Gain**

The available power gain of a two-port network,  $G_A$ , is defined as:

$$G_A = \frac{P_{load,max}}{P_{source,max}}$$

where

$P_{load,max}$  is the maximum available average power at the load

$P_{source,max}$  is the maximum power available from the source

Similarly,  $P_{load,max}$  may only be obtained when the load impedance is the complex conjugate of the output impedance of the network.

The maximum stable gain (MSG) > maximum available gain (MAG), unless the stability factor of transistor = 1.

### **3.1.4 Characteristic Frequencies**

The most important characteristic frequencies of RF devices are the cut-off frequencies ( $f_T$ ), and the maximum frequency of oscillation ( $f_{max}$ ). The cut-off frequency is defined as the frequency at

which the magnitude of  $h_{21}$  (related to the short circuit current gain) goes to unity (or 0 dB). Also, the unilateral power gain  $U$  goes to unity (0 dB).

A rule of thumb is to run the transistor at frequencies that are no more than 50% of the cut-off frequency. For power transistors, this value changes to only a third of the cut-off frequency.

The maximum frequency is the maximum frequency at which the transistor still provides a power gain. It is also the highest frequency at which an ideal oscillator would still be expected to operate. The maximum frequency can be either higher or lower than the cut-off frequency for any given transistor. A general rule of thumb is that  $f_T$  is the most important figure of merit for digital circuits, while  $f_{max}$  is the more important figure of merit for analog applications. However, these ultimately depend on the specific application of the transistor.

### 3.1.5 Noise

Transistors cannot distinguish between signal and noise as it comes in from the input. In other words, an RF transistor will amplify noise just like it will amplify the signal. Besides external noises, there are also noises generated in the transistor. It is very important to keep the noise produced by the transistor as small as possible.

$$\text{Noise figure} = NF = 10\log[(P_{si}/P_{Ni})/(P_{So}/P_{No})]$$

where

$P_{si}$  = signal powers at the input

$P_{So}$  = signal powers at output

$P_{Ni}$  = noise powers at the input

$P_{No}$  = noise powers at output

The magnitude of the NF depends on frequency, bias conditions, and matching conditions at the input of the transistor. It is unfortunate that the best conditions for minimum noise are different than the ones for maximum power gain.

### 3.1.6 Output Power and Power-Added Efficiency

This an important figure of merit for RF transistors used in power amplifiers. For power amplifiers, the amount of RF power that can be delivered is the main concern, and NF is of negligible importance.

When heat dissipation or battery power is of concern, the power added efficiency is an important figure of merit. The power added efficiency (PAE) is defined as:

$$PAE = [P_{out}(rf) - P_{in}(rf)]/P_{in}(dc)$$

where

$P_{out}(rf)$  and  $P_{in}(rf)$  are the transistor's RF input and output powers,

and,

$P_{in}(dc)$  is the dc power delivered by the power supply.

Sometimes the output power is described as an output power density, such as output power per mm gate width in FETs or output power per microns square emitter area in bipolar transistors.

This does not give a figure for the device's total output power, but it provides a good estimate and comparison of the power handling capability of each device, making comparisons across completely different devices a possibility.

### **3.1.7 Mean Time to Failure**

MTTF is an important indication of device reliability. It is an important figure of merit because the device is useless unless it has a long lifetime, or at least long enough for the intended application. One of the problems defining MTTF is defining failure itself. In RF transistors, failure is defined as a degradation in an important performance characteristic of the device. For example, 10% degradation in the current gain is a common failure criteria for HBTs. Sometimes MTTF is defined as degradation in some other important performance criteria, for example, a 15% decrease in the transconductance.

As far as what failure mechanisms contribute to a given MTTF, these vary a lot in RF transistors. In HBTs, degradation can result in stress-induced defects which in turn decrease the current gain. In other types of FETs, degradation can arise from high-electric fields near the drain junction. Gate oxide breakdown is a very common degradation mechanism in CMOS devices, and can be soft or hard breakdown, depending on the quality of the oxide and the interfaces. Device failure and degradation mechanisms specific to RF devices in III-V technology are covered in the next section.

## 4.0 RELIABILITY ISSUES IN RF DEVICES USED IN SPACE APPLICATIONS

### 4.1 General Reliability and Radiation Concerns

The simplest definition of reliability is quality over time. Since time is involved in reliability, it is often measured by a rate. Just as quality is usually measured in terms of rejects (or un-quality), reliability is measured in terms of failures (or un-reliability).

Traditionally, the measurement of electronic failures has been straightforward. If one assumes all failure rates are constant, as they might be in a large system or machine, then a mean time between failures (MTBF) would be expected. In contrast, most integrated circuits, including GaAs devices, follow the lognormal distribution, which rarely approximates a constant rate.

Historically, failure rates were measured in percent failed per thousand hours of operation. The modern unit of failure commonly used today is failure in time (FIT). A FIT is also a unit of failure (or a failure in time) that is equivalent to one failure per billion device hours. For comparison, one FIT is equivalent to 0.0001% per thousand hours, and 1% per thousand hours is equivalent to 10,000 FIT. However, a single rate is not sufficient to describe the reliability of semiconductors since their failure rates change over their lifetimes.

Generally, semiconductors have a very low wear-out failure rate early in life, and then have increasing failure rates as they wear out. At a point when about half of the devices fail in a group of circuits, the failure rate begins decreasing again. A very small part of an integrated circuit's (IC's) population may fail early in life. These early failures have been associated with manufacturing or assembly defects. The early failures are sometimes called "infant mortality" failures. As semiconductor reliability improves and more samples are stressed, the early failures become easier to detect and eliminate.

Failure mechanisms in GaAs device technologies can be significantly different than those observed for traditional Si devices. First of all, the metallization used is primarily composed of gold, which is more conductive than aluminum used in conventional silicon device processing, and is also less susceptible to electromigration. This is because electromigration is a diffusion process; diffusivity scales with the melting point and gold's melting point (1064°C) is much higher than aluminum (660°C). Gold can also be less susceptible to corrosion than aluminum, as it does not form stable oxides. Lastly, gold eliminates the potential for problems with Au/Al intermetallics during assembly since gold bond wires are typically available.

One of the active devices used in mature GaAs ICs is the MESFET. Unlike a Si MOSFET, the gate is formed by a Schottky metal contact to the channel, instead of using a gate oxide. This eliminates the primary failure mechanisms found in MOS devices. Because of this Schottky configuration, the MESFET is relatively immune to surface effects and ionic contamination, which plague silicon devices. In addition, GaAs devices are not susceptible to radiation degradation caused by the sensitivity of gate oxides in Si CMOS devices. Newer GaAs active devices, pHEMTs and HBTs, also have advantages over CMOS devices and similar immunity to typical silicon surface problems.

The last major component of the process is the bulk wafer material itself. GaAs is actually a semi-insulator except in areas where it is implanted with silicon or in epitaxial layers. Because of its higher bulk resistivity, roughly 1,000 times more resistive than silicon, GaAs is much less sensitive to the isolation and latch-up problems associated with silicon and silicon CMOS. There

are other GaAs properties that lend themselves to better reliability, like lower electric fields at peak electron velocity, but they are typically minor issues.

An extended thermal range is another issue regarding reliability of space RF devices. This is not normally a concern in commercial applications like cell phones or laptop computers. In this regard, GaAs has several advantages at both ends of the thermal range. At low temperature, the electron mobility increases, and in good quality, defect-free material is seen to peak at 80 K, so GaAs devices can perform very well at lower temperatures. 80 K is lower than most intended space flight applications. At the high end of the thermal range GaAs also has advantages, since it can be operated safely at much higher temperatures. Some GaAs MESFETs, pHEMTs, and other transistors/diodes can be operated at temperatures up to 300°C.

#### **4.2 Hot Electron Effects**

The hot electron degradation effect is another important degradation mechanism in III-V devices, which is particularly important for devices operated at cryogenic conditions. The traditional temperature acceleration in life testing is more commonly used to predict reliability of GaAs devices, by simply evaluating experimentally the activation energy and then substituting actual use conditions into the Arrhenius equation. The problem with temperature-accelerated stress experiments is that activation energies for GaAs tend to be quite high, and extrapolation to use conditions can give values for predicted MTTF that are too optimistic. One of the reasons is that thermally induced degradation is based on interdiffusion of the different materials involved, and this depends on temperature and not so much on bias conditions. On the other hand, a high-bias stress, related to the hot electron instabilities in the channel, may present a worst case scenario when devices are operated at room or low temperatures in a real environment for a long time period. Such phenomena have been attributed to the formation of deep-level defects generated during hot electron and impact ionization conditions. These are caused by the presence of large electric fields in the device channels and barrier layers. Hot electron effects are quite likely to develop in RF applications (mainly in high electron mobility transistors HEMTs) because in order to be operated at microwave- and millimeter-wave frequencies, the peak channel electric fields are very large even for low drain biases. Hot electron degradation has been shown to cause threshold voltage shifts, breakdown walk out, transconductance and cutoff frequency degradation, and the so called “power slump.”

#### **4.3 Radiation Tolerance of RF Devices**

Understandably, there is a large number of studies on the effects of space radiation on GaAs based solar cells, and a lesser number on GaAs-based, light-emitting diodes. GaAs-based RF devices have not been the subject of as many studies. One of the reasons is that it is very difficult to degrade GaAs-based RF devices with radiation; they are viewed as “radiation hard,” and are considered robust for many space applications.

From a device point of view, we have three radiation-induced phenomena:

*Effects from total ionizing dose (TID).* These originate from ionizing radiation damage induced by incident charged particles: protons, electrons, or photons.

*Displacement damage (DD) effects.* There can be displacement damage on the semiconductor crystal lattice related to incident particle interactions with the semiconductor lattice atoms. Heavier energetic particles can cause knock on damage, or displacements that cause defects.

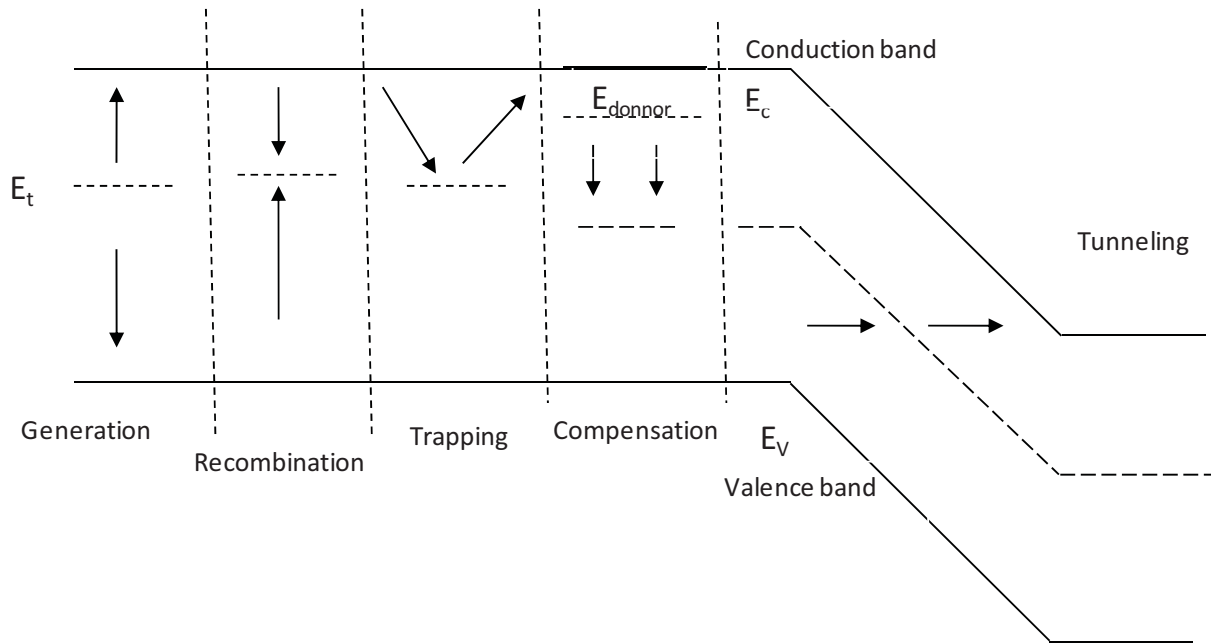


**Figure 4.3-1.** Illustration of some basic effects of a defect energy level ( $E_t$ ) on the electrical performance of a device. Displacement damage introduces deep levels in the semiconductor bandgap [12].

These defects are any deviation from perfect lattice periodicity (interstitials, vacancies, anti sites, others). This is associated with the volume of devices and can result in deactivation of dopants (carrier removal) as well as degradation of carrier lifetime, mobility, and diffusion lengths. Some of the effects of radiation-induced defects are graphically illustrated in Figure 4.3-1. Carried to an extreme, at very high fluences, displacement damage can be so severe that the crystal lattice becomes amorphous, or completely disordered.

*Single-event effects (SEE).* These are associated with very high energy particles, protons, and neutrons of high atomic mass cosmic rays. This type of ionization damage in devices has involved the isolating oxides, also the oxide to semiconductor interfaces. It is thus usually relevant to device surfaces and interfaces. Cosmic ray induced SEE are often associated with data loss or error generating phenomena in switching circuits, and they are considered “soft errors.” Even GaAs devices suffer from poor single-event upset (SEU) immunity at high data rates. Tolerance or hardness to SEU sometimes requires new design architectures, so “radiation hardening by design” can be achieved.

Protons are considered the worse case for radiation effects since they produce both ionizing and displacement damage. Radiation from energetic protons in space usually comes from three main sources: (i) the Van Allen radiation belts, (ii) solar proton events/solar energetic particles, and (iii) galactic cosmic rays. Van Allen radiation belts have many protons in the energy range of 1–10 MeV. There are higher energy protons out there, but at much smaller fluences. Most of the protons that electronic devices are likely to encounter in space are in the 1–10 MeV range.

Testing for radiation effects is traditionally done at around 100 MeV, 50 MeV, 10 MeV, and 1–2 MeV. The energy used in most of the radiation reports on RF devices (mostly on different types of HBTs) is 46 MeV. This indicates an important gap in the data, and more need for radiation testing with protons in the range 1–10 MeV. Since high energy protons are less damaging because they deposit less energy in the active region of the device, testing only with protons

around 50 MeV could give deceptively optimistic results. More testing should be carried out at the lower proton energies, which are known to be more damaging to the active areas of HBTs and other GaAs devices.

“Carrier removal” is an effect seen at the intermediate stages of radiation damage in devices. As discussed in previous sections, doping is essential in the fabrication of any transistor device. The doping will achieve a certain carrier concentration, either of electrons or holes. These are from shallow impurities, which are all ionized at room temperature and electrically active as either n or p type dopant impurities. When radiation introduces displacement damage defects, these defects have energy levels that are somewhere near the middle of the semiconductor bandgap. If the concentration of these defects becomes comparable to the original doping concentration, the Fermi level becomes pinned closer to the middle of the bandgap, compensating the shallow donors (or acceptors). The measured resistivity increases, or the carrier concentration (as measured by standard techniques like Hall effect) diminishes. This is why the phenomenon is known as “carrier removal.” As would be expected, changing the effective carrier concentration in the active parts of the device will also change its performance characteristics.

Numerous studies have been carried out over the years on the effects of ionizing radiation on Si devices. In comparison to compound semiconductors, Si-based devices degrade significantly with ionizing radiation. Si BJTs have shown severe degradation with a few tens of krad dose exposure. Damage to the emitter base space oxide degrades the base current, leading to current gain collapse. The effects of displacement damage lead to increased base resistance (due to carrier removal), decreased carrier lifetime, and dynamic response degradation. These problems have a serious impact on circuit performance even at modest radiation levels. Scaling to smaller sizes has somewhat improved this scenario by decreasing device volumes and volumes of sensitive areas.

A study comparing the effects of gamma irradiation on SiGe and GaAs HBT technologies [13] showed that both SiGe and GaAs HBT technologies are tolerant to gamma radiation up to 1 Mrad(Si). Gamma radiation does not cause displacement damage though. The authors in the aforementioned study measured effects on DC and RF performance as well as their low frequency noise, and they did observe more degradation in low frequency noise from the GaAs HBT devices.

There has been significantly more research on radiation effects on SiGe HBTs, which encompasses effects of electron, proton, neutron, and gamma irradiation on these devices. The fewer studies done on the III-V devices show good promise for radiation hardness in GaAs and InP-based HBTs, and even greater hardness for the GaN-based devices. Some of the additional work that has been done on these RF materials systems includes the effects of proton irradiation on AlGaAs/GaAs HBTs [14], GaN HEMTs [15], and AlGaN/GaN HEMTs [16]; and the effects of neutron, proton, and electron irradiation on InGaP/GaAs HBTs [17].

Among the several findings of the effects of space radiation on SiGe HBTs [18, 19–20] were that response to proton radiation at different 46 MeV proton fluences ( $10^{12}$  to  $10^{14}$ ) results in a diminished current gain at low collector currents. However, these conditions are the equivalent to a gamma dose of over 1.5 Mrad(Si), which is a higher dose than what most orbital missions will be exposed. The base current in these irradiated devices increases due to the creation of trapping centers; hence, the current gain of the device deteriorates. Even though there is a measurable degradation, the peak current gain in these devices does not show much degradation, since it

takes  $10^{14}$  proton/cm<sup>2</sup> to degrade it by less than 10%. This performance under proton radiation compares very favorably with the silicon BJTs and other devices.

As far as AC performance, none of the 4 s parameters suffered significant degradation even after proton fluence of  $1 \times 10^{14}$  protons/cm<sup>2</sup>. The cutoff frequency and oscillation frequencies were barely changed even after  $5 \times 10^{13}$  protons/cm<sup>2</sup>, despite the fact that there are radiation-induced traps in the collector. Even though radiation traps (deep-level defects) were found, they were not in sufficient concentrations to cause significant carrier removal or a significant decrease in the device's carrier concentration.

Comparison of SiGe HBTs and Si BJTs fabricated identically but using Ge in the base were carried out. It was found that the Ge material is not responsible for the increase in radiation tolerance to TID. Research on this issue indicates that the reason for the increased tolerance of SiGe devices is due to the higher doping of the extrinsic base region, the emitter base spacer is thinner and made of a more resistant oxide/nitrite composite, and the active volume of these transistors is extremely small, lessening the impact of displacement damage.

Studies focusing on the effects of energetic protons on III-V compound HBTs show good promise for the radiation hardness of these materials. In one of the few studies where the effects of lower energy protons (1.8 MeV) on HBTs were investigated, a study of AlGaAs/GaAs HBTs proton-induced degradation [14] used both 1.8 MeV and 105 MeV protons. This paper shows how much more damaging 1.8 MeV protons are to the device gain. This is because 105 MeV protons have much lower non-ionizing energy loss (NIEL) in the sensitive region of the device. In other words, high-energy protons are less damaging because they deposit less energy in the active region of the device. Degradation of the AlGaAs/GaAs HBTs was caused by an increase in the base current and a decrease in the collector current. For these devices, NIEL is more relevant than total ionizing dose. No degradation due to TID total ionizing dose was found. Fluences were from  $3 \times 10^{11}$  up to  $3 \times 10^{13}$ /cm<sup>2</sup> for both proton energies. Gain decreases significantly after 1.8 MeV proton irradiation; almost no effect from 105 MeV protons though. This is because NIELS is 70 times higher for the first two microns of the device with 1.8 MeV than 105 MeV protons.

The effects of proton irradiation-induced defects on GaN HEMTS performance [15] were also investigated; it was found that defects degrade both the charge in the 2-deg and the electron mobility. 1.8 MeV protons induced defects that also caused gate lag, which is the delayed response of the device to a change in gate voltage on AlGaN/AlN/GaN HEMTs. Both bulk and surface state defects have been associated with this gate lag. The authors of this study were able to simulate pre-irradiation gate lag from surface states or surface defects. They found that only with significant introduction of bulk defects produced from proton irradiation into the AlGaN and GaN protons do these degrade further. The high fluence of protons required to induce these changes confirms that GaN is radiation hard and suitable to operate in space environments.

1.8 MeV protons were also used to test radiation hardness of AlGaN/GaN [16] high electron mobility transistors. This work showed that contact resistance can degrade for fluences  $10^{11}$  to  $10^{14}$  protons/cm<sup>2</sup>, and that degradation of the channel properties occurs when the proton fluences are even higher. Minimal changes in both saturation current and transconductance were not observed until fluences exceeded  $10^{13}$  p/cm<sup>2</sup>. Device parameters were unaffected at levels up to  $10^{13}$  fluences; small effects were seen at  $10^{14}$  protons/cm<sup>2</sup>. Serious degradation effects were not measured up to  $10^{15}$  protons/cm<sup>2</sup>. This work shows the extreme radiation hardness that the

devices based on nitride compounds can exhibit. For comparison, GaAs HEMTs show about 20% decrease in drain current after 2 MeV proton fluence of  $3 \times 10^{12}$  protons/cm<sup>2</sup>. This is equivalent to two orders of magnitude lower fluence than is required to achieve similar degradation in GaN HEMTs. Effects include some Schottky barrier height variation and some changes in the current-voltage characteristics (gate I vs. gate V). In contrast, ohmic contact degradation in GaN is significant for fluencies of  $10^{12}$  for equivalent proton energy. The DC characteristics were found to be very radiation tolerant, since the mobility in the device channel did not degrade until proton fluences reached  $10^{14}$  protons/cm<sup>2</sup> and sheet density did not degrade until fluences of  $10^{15}$  protons/cm<sup>2</sup>. Changes in the electrical contacts were observed for relatively low fluences, indicating that ohmic contact degradation might be the weakest link in the HBT nitride reliability.

In a recent study of radiation effects in InGaP/GaAs HBTs [17], comparisons were made between the effects of neutron (100 KW), proton (67 or 105 MeV), and electron irradiation (1 MeV). This study found the degradation to be very dependent on particle type, energy, and fluence. Advantages of InGaP/GaAs over AlGaAs/GaAs include higher valence band offset to suppress back injection of holes in the emitter, better etch selectivity between the heterojunctions (InGaP and GaAs), lower surface recombination velocity, absence of DX centers, and better long term reliability. InGaP/GaAs HBTs were found to be radiation hard for electron fluences greater than  $10^{15}$  electrons/cm<sup>2</sup>, proton fluences up to  $10^{12}$ /cm<sup>2</sup>, and neutron flux greater than  $10^{13}$ /cm<sup>2</sup>, since the devices exhibited only modest degradation up to those fluences. At low fluence of proton and neutron irradiation, these devices actually show a small increase in gain. They did compare different emitter sizes and devices fabricated with two different growth techniques. Gain degradation at higher fluences was found to be due to displacement damage in the emitter-base region.

#### **4.4 Quantifying Degradation in Life Tests**

One non-trivial issue is defining failure. In some cases, failure is straightforward; the device fails completely and cannot function at all. This is what is known as catastrophic failure. However, in many cases failure is not so clear cut, mainly, if the device has suffered significant degradation but has not failed completely. It will still work, but some of its performance characteristics, as defined in a data sheet for example, degrade to some percentage of its original performance specifications. For many applications, failure is defined as a somewhat arbitrary percentage degradation in one or more of the relevant performance parameters. A decrease in 10%, 15%, or 20% in the gain (known as beta  $\beta$ ) or transconductance are common criteria for failure when no catastrophic failure is observed; but degradation in other device parameters are also used.

In real-life space applications, oftentimes the modes of failure or device degradation are varied and the failure mechanisms are extremely complicated. This is why many life tests are performed empirically. Prolonged life tests in RF devices are performed for the RF devices deployed in space applications much after the launch dates, and these are continued even after the flight mission is in progress. Experience has shown that this is the best way to obtain data from the RF devices of interest.

#### **4.5 Modes of Failure in RF Devices**

Common failure mechanisms in GaAs-based devices include interdiffusion [21]. The primary failure mechanism for MESFET pHEMT ICs and HBTs are “sinking gates.” Sinking gates are

caused by gate metal interdiffusion into the channel. This interdiffusion causes parametric shifts in several device parameters because the effective channel thickness is reduced. The largest change that gate sinking causes is decreased channel current. This is why this parameter is typically used as the failure criterion: a 20% change in channel current is a common definition of a MESFET failure. In addition to channel current changes in an FET with sinking gates, channel resistance increases and the magnitude of the voltage required to pinch-off an FET is reduced (this usually means pinch offs are more positive). Sinking gates have never been catastrophic and they are self-limiting in a sense, because as the channel current decreases so does the power in the FET and thus the temperature is lowered causing the gates to sink more slowly. Eventually, one could expect the channel to be severed completely by the gate and become open, but this condition is rarely reached. The sinking gate mechanism has been observed at various temperatures and biases, but degradation is accelerated by temperature without bias or RF drive.

Gate degradation can be observed using cross-sections formed with a focused ion beam (FIB). The movement of the metal gate at the GaAs surface is dramatic after high temperature aging. Some metal voiding is also present in the degraded gate, because of the mass of material that has moved into the GaAs. Operation at the maximum rated temperature (150°C) would be expected to exceed 2,000 years before a 1dB change could be observed. This expected longevity of sinking gates is acceptable in terms of commercial reliability goals, and is not considered a threat to device lifetimes under normal operating conditions. Although gate sinking can be induced by high temperature acceleration, it has not yet been observed under nominal use conditions.

The failure mechanism for first-layer interconnect begins with an interdiffusion mechanism. The interconnect is composed of a layered structure of titanium, platinum, and gold. When these metals interdiffuse, the resistance of the interconnect increases. Auger studies indicate that the metals intermix, and the whole stack becomes homogeneous. On a percentage basis, the resistance change can be as high as 250%. But on an absolute basis, a 50% change is roughly as much as the process window is wide, or 40 milli-ohms per square cm.

Implanted resistors have been studied to evaluate Ohmic contact failure mechanisms, but Ohmic degradation mechanisms have been elusive. Implanted resistor degradation has been found to be caused by changes in the contact resistance. Failure analysis on degraded FETs has shown that Ohmic metal does diffuse into the GaAs, but the physical diffusion seems to have a minimal effect electrically on the FET performance, especially compared to sinking gates. In general, Ohmic annealing is beneficial to circuit performance.

Other types of degradation mechanisms have been found for SiGe HBTs. In a study of SiGe HBT reliability issues [18] for mixed-signal circuit applications, it was found that in addition to device reliability mechanisms associated with reverse emitter-base and high forward current density stress, there were new reliability issues for SiGe HBTs. These include impact-ionization stress, scaling-induced breakdown voltage compression, operating point instabilities, geometrical scaling-induced low-frequency noise variations, and impact of ionizing radiation. Mixed-mode degradation is a “new” degradation mode or reliability “issue” found in SiGe devices.

These devices are primarily used as intermediate frequency (IF) for millimeter-wave applications, and they have shown a dramatic rise in device-level performance since the first generation of such devices. They are also extensively used in mixed-signal applications, which means integration of analog RF functionality with digital circuit functionality within the same IC technology. The peak beta increased from 100 to 400, and the peak unity gain cut-off frequency

went from about 50 GHz to over 200 GHz from the first to the third generation of such devices. In 2006, the frequency maximum was over 300 GHz (it was 285 GHz in 2004). Increased reliability issues and concerns go hand in hand with increases in performance, and SiGe HBT technology is no exception.

Self heating has also been identified as a reliability concern in SiGe HBTs [22], where simulations showed an increase in electron mobility and saturation velocity in npn SiGe HBTs. It was found that an increase in the base-collector depletion layer width degrades the  $f_T$  while increased base resistance also contributed to the reduction in  $f_{max}$ . The onset of significant device self-heating and degradation in  $f_T$  and  $f_{max}$  were observed for collector current densities of  $5 \times 10^4$  A/cm<sup>2</sup> for  $V_{CE} = 2$  V.

In another recent study [23], electrical stress has been seen to cause degradation in the DC current gain in SiGe HBTs. They investigated hot carrier effect in 35 GHz maximum frequency devices. They demonstrated degradation due to hot electrons by applying a high collector current density and high collector-base voltage, to simulate mixed-mode stress.

#### 4.6 Electrostatic Discharge Failures

Electrostatic discharge (ESD) has been the leading cause of failure in the field, and ESD failures scale inversely with device size. Therefore, efforts to reduce ESD sensitivity by design and handling countermeasures will become increasingly more important as device sizes continue to decrease.

The problem is difficult to model and analyze since the various sources of electrostatic energy—such as the human body, testing equipment, and accumulated free charge—all have different electrical characteristics. In addition, the abrupt and intense nature of a typical ESD event forces the devices that absorb the discharged energy to operate under high injection conditions, where the analysis is quite complex. Providing adequate protection against ESD also requires effective thermal distribution within the discharge area in order to avoid dielectric damage, semiconductor melting, or metal spiking. To address these issues appropriately, each pad must be protected by a device capable of sustaining the discharged energy with no internal damage, preferably without compromising process complexity, total chip size, and electrical performance.

#### 4.7 Electromigration

While metal/semiconductor interdiffusion is the most common wear-out mechanism, and occurs in GaAs contacts, interconnects, and resistors, electromigration is another common failure mechanism that also occurs in interconnects and resistors. If life testing is conducted under bias, electromigration can eventually occur, which causes catastrophic open circuits.

The failure mechanism for plated-gold interconnect and air bridges in MMICs is electromigration. Under high-current density stress, mass transport occurs because of the “electron wind” in the metallization. Voids form along the plated gold, and eventually the interconnect fuses open, the nitride passivation will crack, and molten gold will flow out of the failure site. Less than a 25% change in plated-gold resistance has ever been observed before the catastrophic failure, and usually the pre-fusing degradation is negligible.

## 4.8 Other Failure Modes

Life tests for the different HBT materials have given activation energies, so Arrhenius dependences can be assumed and MTTF predicted. Under this scenario, activation energies can be extracted from MTTF (in hours) vs.  $1/KT$ . InGaP/GaAs HBTs have shown activation energies around 2 eV, whereas life tests on AlGaAs/GaAs HBTs have given activation energies as low as 0.6 eV under the same conditions. Changes in base and or collector currents are also taken as a measure of device degradation/failure.

Other possible (less common) failure mechanisms are surface charge effects, leakage effects, ohmic contact degradation, burn-out, channel compensation, Schottky contact degradation, carrier diffusion, substrate via cracking, side-gating, gate electromigration, passivation cracking, interconnect-air-bridge contact degradation, hydrogen-gate interdiffusion, capacitor dielectric breakdown, inter-level dielectric breakdown, and Ohmic contact electromigration.

## 4.9 Issues in Space RF Reliability

A good description of qualification methodologies for GaAs MMICs can be found in a journal article summarizing most of the JPL GaAs MMIC reliability assurance guideline for space applications [24] where qualification methodologies are discussed, and the various acceptance tests targeted for space qualification are described.

A common problem encountered during some space qualifications of RF devices, where MTTFs are to be predicted for one-of-a-kind type RF devices is that there are often too small sample sizes to adequately predict reliability under use conditions. The statistical significance of reliability analysis is directly related to the sample size used in the various stress tests. Small sample sizes often force the reliability engineer to waive some of the stress tests, which is not an optimal situation, especially in high reliability space applications.

Another problem that reliability engineers often encounter is the lack of failures. Paradoxically, this is a very undesirable situation. It is essential to know how devices will fail under use conditions. This is the first key question that leads to understanding reliability. Failures are considered to be an essential part of each reliability study. Failures are required to identify root causes of reliability problems, or to evaluate the weakest link of device so that improvements can be made for the best impact on reliability. Failures also provide the reference point for future comparisons. If subsequent tests are run before and after a process change, and they both result in zero failures, there is no way to decide if the process change improved or impaired the reliability. Most importantly, without a failure, a failure distribution cannot be determined.

Oftentimes, it is necessary to understand failure mechanisms that affect each element of a circuit, but this is not possible if ICs are tested as a whole, since only failure through the weakest link will occur. Some of the other failure mechanisms might be important to understand, but their onset in ICs is too slow to be observed compared to the most predominant failure. In order to measure various failure mechanisms, it is often necessary to break the ICs into elements in order to study various component parts on an individual basis. By breaking ICs into these individual parts or test structures, the failure mechanisms that uniquely affect each element are more easily identified and studied.

To predict MTTFs once test structures or devices are available, activation energies and acceleration factors can be determined for several uses and stress conditions. A few examples are current stressing, thermal stressing, a combination of current and thermal stressing, and testing in

humid environments to assess effects of non-hermetic packages. These stress tests need to be done after setting up “failure criteria,” which specifies the percentage of degradation (10% to 20% degradation are typical; sometimes it can be as high as 50%). For Ohmic contacts, the definition of failure could be, for example, an increase of 50% or more in contact resistance. For Schottky junctions, increase in leakage current is usually observed upon stressing, and sometimes an increase in the diode ideality factor. Therefore, “failure” can be defined as an increase in leakage current of one or two orders of magnitude over the unstressed values. In space applications, these “failure” criteria are often determined based on mission requirements.

#### **4.10 Space Qualification and Use of RF Devices—Recommendations**

- Developing the test infrastructure required to life-test RF devices on site is very important. The challenge here is the need for speed testing at RF frequencies. This allows changing the conditions of the test to adjust to special conditions in space applications. One of the needs for infrastructure development, which is common to many devices and structures, is the implementation of digital data acquisition in real time. Development of the required software, hardware, and instrumentation is needed to perform the tests described here. Furthermore, the experience acquired and testing facilities developed are also instrumental in supporting flight project needs in future testing of RF devices. Theoretical background, software (SPICE and others), analytical skills, and failure analysis tools allow these special tests. Instrumentation and expertise in RF device characterization are needed to determine how different aging schemes like elevated temperature, electrical bias, corroding/oxidizing atmospheres, operation in cold or hot conditions, thermal cycling, or others affect device performance.
- As noted in this report, there are many reasons why gallium arsenide and gallium arsenide-based devices can have good reliability, but the primary cause is that quality and reliability is built into the process. Each GaAs manufacturer has a different “recipe” for the fabrication of devices, and each manufacturer has different strengths and weaknesses. In part selection, RF devices should be procured from manufacturers that share data from their reliability studies.
- For cryogenic applications of GaAs devices operated in RF conditions, hot electron effects are significantly more relevant to real-use conditions. GaAs device manufacturers do not typically perform these studies as part of device qualification; however, hot electron effects tests can provide a more accurate assessment of reliability in space applications; therefore, they should be performed in space qualification of RF devices. This is even more important if the devices are to be used at cryogenic temperatures.
- The evaluation of junction temperature during operation is very important. In hybrid circuits, the hottest element should be identified. Knowing potential temperature gradients in devices during operation is also important, and it can be a reliability concern in space use of GaAs RF devices. This evaluation can be performed using infrared (IR) imaging or cathodoluminescence (CL) spectroscopy/imaging, for example. Determination of the effects of thermal gradients on device reliability is a logical follow-up.
- Cryogenic infrastructure and expertise should be established. This allows filling the testing “hole” from industrial partners. Even if manufacturers share data, they usually do not test at the cryogenic temperature that devices will see in many present and future missions.

#### 4.11 Studies Relevant to Space Use of RF Technology—Recommendations

- An important issue in microwave devices is the extrapolation of DC electrical characteristics in predicting RF performance. This is a complex issue, and device physicists find that among several “good” devices that exhibit similar DC electrical characteristics (current vs. voltage is primarily used), there can be large variations in their RF performance. Since high-frequency testing is more difficult, expensive, and requires special set-ups, finding a way to correlate good high-frequency characteristics with some measurable (DC) parameter would be a major breakthrough in the areas of microelectronics reliability and device characterization.
- As mentioned in the radiation effects section, effects of energetic protons on III-V HBTs and other transistors should include more testing within the 1 MeV to 10 MeV range, because more damage is expected from these lower energy protons. Protons at the energies 1 MeV–10 MeV are abundant in space.
- More annealing studies are needed. Traps that are induced by TID or displacement damage from energetic electrons, protons, and neutron fluxes can be annealed. This means that the density or concentration of these radiation-induced defect levels can be diminished. As explained here, these defects have a detrimental effect on device performance. Part of this performance can then be recovered if some of the defects are removed by annealing. Performing annealing studies would allow accurate experimental determination of temperatures, times, and electrical biases, optimized for each RF device in space applications. Mitigation schemes can then be implemented with this information.
- Studies including radiation effects at low temperatures in RF devices are also needed, given the planned flight missions to cold radiation environments. It is also known that while some radiation-induced defects can be annealed at room temperature, such annealing will not occur if these devices are irradiated at cryogenic temperatures, as is expected in the space environment near the Jovian moons. Experiments using ion implantation at liquid nitrogen temperatures have shown amorphization of crystalline structures while a similar implantation dose does not have as strong an effect and does not make the semiconductor amorphous. Once a semiconductor becomes amorphous, annealing of the structure can no longer repair it.
- Studies of contact resistance with different candidate metal schemes at low temperatures could answer the questions: Are standard Au/Ge/Ni/Ag/Au Ohmic contacts optimized for devices operating at low temperature? Is there a better or more reliable metallization scheme for low temperature Ohmic contacts to GaAs?
- Since most of the NASA applications for GaAs varactors and mixer diodes are based on the characteristics of rectifying metal/semiconductor contacts, more is learned in studies that isolate the simplest device components and avoid design complications. The key device components are the Ohmic contacts and the Schottky junctions. GaAs devices targeted for THz applications use the same type of metallization for Ohmic and Schottky contacts. Ohmic contacts are made of Au/Ge/Ni/Ag/Au, and Schottky contacts are made of Ti/Pt/Au. There is promising work using Pd/Ge/Au as Ohmic contacts. For Schottky junctions, Al has given very high barrier heights in GaAs, and diffusion of Al into GaAs does not cause deep levels. Therefore, these two alternate metallization schemes have been proposed for comparative reliability studies. Fabrication and testing of test structures should be carried for Ohmic contacts of GaAs (at least two types of test

structures, the transmission line method and the Kelvin cross structure), and for Schottky or rectifying junctions and contacts on GaAs.

- The most common failures are the result of metal/semiconductor interdiffusion; radiation is known to enhance diffusion. How would radiation damage then affect life-testing results? Are there any synergistic effects from radiation and aging in long-term use conditions? Does this mean that our life test results, and the activation energies found for different devices, could be different when the device is operated for months or years in a radiation environment? Studies examining this possible synergy are needed to answer these questions.

## 5.0 REFERENCES

- [1] Sze, S. M., *Semiconductor Devices, Physics and Technology*, John Wiley & Sons, Inc. 1985.
- [2] Kroemer, H., “Quasi-Electric and Quasi-Magnetic Fields in Non-Uniform Semiconductors,” *Symposium on the Role of Solid State Phenomena in Electric Circuits*, Polytechnic Institute of Brooklyn, pp. 143–153, 1957, re-published in *RCA Review*, vol. 18, pp. 332–342, 1957.
- [3] Fukano, H., Y. Itaya, and G. Motosugi, “InGaAs/InP Heterojunction Bipolar Transistor with High Current Gain,” *Japanese Journal of Applied Physics*, vol. 25, pp. L504–L506, 1986.
- [4] Kashio, N., and K. Kurishima, Y. Fukai, M. Ida, and S. Yamahata, “High speed and high-reliability InP based HBTs with a novel emitter,” *IEEE Trans. Electr. Devices*, vol. 57, p. 373, 2010.
- [5] Ando, T., “Theory of Hall-effect in a 2-dimensional electron-system,” *Jour. Phys. Soc. Japn*, vol. 39, p. 279, 1975.
- [6] Perret, J., and J. Skinner, “Report on the TI RF Characterization Task,” Interoffice Memorandum, 5140-05-279, 2005.
- [7] Srinivasan, D. K., M. E. Perry, K. B. Fielhauer, D. E. Smith, and M. T. Zuber, “The Radio Frequency Subsystem and Radio Science on the MESSENGER Mission,” *Space Sci Rev*, vol. 131, pp. 557–571, 2007.
- [8] Stanley, S., K. Ho, and C. E. Saavedra, “A CMOS Broadband Low-Noise Mixer with Noise Cancellation” *IEEE Transactions on Microwave Theory and Techniques*, vol. 58, no.5, pp. 1126–1132, May 2010.
- [9] Schwierz, F., and J. Liou, “Semiconductor devices for RF applications: evolution and current status,” *Microelectronics Reliability*, vol. 41, pp. 145–168, 2001.
- [10] Itoh, Y. and K. Honjo, “Recent advances in Measurement techniques for microwave active devices and circuits,” *IEICE Trans. Electron*, vol. E87-C, p. 657, 2004.
- [11] Kurokawa, K., “Power waves and the scattering matrix,” *IEEE Trans. on Microwave Theory and Techniques*, vol. 13, p. 194, 1965.
- [12] Srour, J. R., and J. M. McGarrity, “Radiation effects on microelectronics,” *IEEE Trans Nucl Sci*, vol. 76, pp. 1443–1469, 1988.
- [13] Zhang S. M., “A comparison of the effects of gamma irradiation on SiGe HBT and GaAs HBT technologies,” *IEEE Transactions on Nuclear Science*, vol. 47, p. 2521, 2000.
- [14] Hu, X., B. Choi, H. Barnaby, D. Fleetwood, R. Schrimpf, K. Galloway, R. Weller, K. McDonald, U. Mishra, and R. Dettmer, “Proton induced degradation in AlGaAs/GaAs Heterojunction Bipolar Transistors,” *IEEE Trans. on Nuclear Science*, vol. 49, p. 3213, 2002.
- [15] Kalavagunta, A., M. Silvestri, M. Beck, S. Dixit, R. Schrimpf, R. Reed, D. Fleetwood, L. Shen, and U. Mishra, “Impact of Proton Irradiation-induced bulk defects on Gate-Lag in GaN HEMTs,” *IEEE Trans. on Nuclear Science*, vol. 56, p. 3192, 2009.
- [16] White, B., M. Bataiev, S. Goss, X. Hu, A. Karmarkar, D. Fleetwood, R. Schrimpf, W. Schaff, and L. Brillson, “Electrical, Spectral, and Chemical Properties of 1.8 MeV Proton Irradiated AlGaIn/GaN HEMT Structures as a Function of Proton Fluence,” *IEEE Trans. on Nuclear Science*, vol. 50, p. 1934, 2003.

- [17] Vuppala, S., C. Li, P. Zwicknagl, and S. Subramanian, "Neutron, Proton, and Electron Irradiation Effects in InGaP/GaAs Single Heterojunction Bipolar Transistors," *IEEE Trans. on Nuclear Science*, vol. 50, p. 1846, 2003.
- [18] Cressler, J. D., "Emerging SiGe HBT reliability issues for mixed-signal circuit applications," *IEEE Transactions on Device and Materials Reliability*, vol. 4, pp. 222–236, 2004.
- [19] Roldan, J., G. Niu, W. Ansley, J. Cressler, and S. Clark, "An investigation of the spatial location of proton-induced traps in Si/Ge HBTs," *IEEE Trans. Nuclear Science*, vol. 45, pp. 2424–2430, 1998.
- [20] Zhang, S., G. Niu, S. Clark, J. Cressler, and M. Palmer, "The effects of proton irradiation on the RF performance of SiGe HBTs," *IEEE Trans. Nuclear Science*, vol. 46, pp. 1716–1721, 1999.
- [21] Ueda, O., "Reliability issues in III-V compound semiconductor devices: optical devices and GaAs based HBTs," *Microelectronics Reliability*, vol. 39, p. 1839, 1999.
- [22] Sampathkumaran, R., and K.P. Roenker, "Effects of self-heating on the microwave performance of SiGe HBTs," *Solid State Electronics*, vol. 49, p. 1292, 2005.
- [23] Huang, S., K. Chen, G. Huang, C. Hung, W. Liao, and C. Chang, "Electrical stress effect on RF power characteristics of SiGe hetero-junction bipolar transistors," *Microelectronics Reliability*, vol. 48, pp. 193, 2008.
- [24] Kayali, S., "Reliability of compound semiconductor devices for space applications," *Microelectronics Reliability*, vol. 39, p. 1723, 1999.

## APPENDIX A. AVAILABLE DEVICES

Table A-1. Low noise amplifier industry survey, devices available as of 2005.

item	manufacturer	device	technology	freq range (GHz)	noise figure (db)	gain	power supply (Volts)	power supply (mAmps)	DC power (mWatts)	package	available as die	T <sub>OP_MAX</sub> °C	T <sub>OP_MIN</sub> °C	T <sub>ABS_MAX</sub> °C	T <sub>ABS_MIN</sub> °C
1	Celeritek	CF007-01	GaAs FET	2 - 20	2.2	11.5	4.0	25	100	---	yes			+175	-65
2	Eudyna	FHX04X	GaAs HEMT	2 - 18	0.9	10.5	2.0	10	20	---	yes	+80		+175	-65
3	Celeritek	CF001-03	GaAs P-HEMT	2 - 26	1.2	15.0	3.0	15	45	---	yes			+175	-65
4	TriQuint	TGF4350-EPU	GaAs P-HEMT	0 - 22	1.2	14.5	3.0	15	45	---	yes			+150	-65
5	Celeritek	CF003-03	GaAs P-HEMT	2 - 26	1.4	18.0	3.0	30	90	---	yes			+175	-65
6	NEC	NE67400	GaAs MESFET	2 - 12	0.6	14.0	3.0	10	30	83B	yes			+175	-65
7	NEC	NE71300	GaAs MESFET	0 - 12	0.6	14.0	3.0	10	30	---	yes			+175	-65
8	TriQuint	TGF1350-SCC	GaAs MESFET	0 - 18	1.5	11.0	3.0	15	45	---	yes			+150	-65
9	NEC	NE321000	AlGaAs Si- P-HJ FET	2 - 12	0.4	13.5	2.0	10	20	---	yes			+175	-65
10	NEC	NE27200	AlGaAs/InGaAs Si- HJ FET	2 - 12	0.5	12.5	2.0	10	20	---	yes			+175	-65
11	<b>NEC</b>	<b>NE32500</b>	<b>AlGaAs/InGaAs Si- HJ FET</b>	<b>2 - 12</b>	<b>0.5</b>	<b>12.5</b>	<b>2.0</b>	<b>10</b>	<b>20</b>	<b>---</b>	<b>yes</b>			<b>+175</b>	<b>-66</b>
12	Filtron	FPD200	AlGaAs/InGaAs P-HEMT	0 - 12	1.1	17.0	5.0	30	150	---	yes			+175	-40
13	NEC	NE68000	Si BJT	0 - 4	1.7	12.5	6.0	5	30	SOT-343	yes			+150	-65
14	NEC	NE68100	Si BJT	0 - 4	1.6	12.0	8.0	7	56	SOT-343	yes			+150	-65
15	Agilent	AT-41400	Si BJT	0 - 6	1.6	14.5	8.0	10	80	---	yes			+200	-65
16	<b>Sirenza Microdevices</b>	<b>SGA-8300</b>	<b>SiGe HBT</b>	<b>0 - 6</b>	<b>1.2</b>	<b>16.5</b>	<b>3.0</b>	<b>10</b>	<b>30</b>	<b>---</b>	<b>yes</b>			<b>+150</b>	<b>-40</b>
17	Eudyna	FSU01LG	GaAs FET	0 - 3	0.5	18.5	3.0	10	30	LG case	no	+145		+175	-65
18	Eudyna	FSU02LG	GaAs FET	0 - 3	1.5	17.5	3.0	20	60	LG case	no	+145		+175	-65
19	Sirenza Microdevices	SPF-3143	GaAs P-HEMT	0 - 10	0.9	15.1	3.0	20	60	SOT-343	no			+150	-40
20	<b>NEC</b>	<b>NE34018</b>	<b>GaAs HJ FET</b>	<b>1 - 3</b>	<b>0.6</b>	<b>16.0</b>	<b>2.0</b>	<b>5</b>	<b>10</b>	<b>SOT-343</b>	<b>no</b>			<b>+125</b>	<b>-65</b>
21	<b>NEC</b>	<b>NE52418</b>	<b>GaAs HBT</b>	<b>0 - 7</b>	<b>1.0</b>	<b>17.0</b>	<b>2.0</b>	<b>3</b>	<b>6</b>	<b>SOT-343</b>	<b>no</b>			<b>+125</b>	<b>-65</b>
22	Infineon	BFP740F	SiGe BJT	0 - 10	0.5	19	3	25	75	TSFP-4	no			+150	-65
23	NEC	2SC5761	SiGe BJT	0 - 4	0.9	18.0	2.0	5	10	M04	no			+150	-65
24	<b>Sirenza Microdevices</b>	<b>SGA-8343</b>	<b>SiGe HBT</b>	<b>0 - 6</b>	<b>1.2</b>	<b>16.5</b>	<b>3.0</b>	<b>10</b>	<b>30</b>	<b>SOT-343</b>	<b>no</b>			<b>+150</b>	<b>-40</b>
25	Sirenza Microdevices	SGA-9289	SiGe HBT	0 - 3	3.3	10.8	3.0	162	486	SOT-343	no			+150	-40
26	Sirenza Microdevices	SGA-9189	SiGe HBT	0 - 3	3.9	11.1	3.0	108	324	SOT-343	no			+150	-40

Table A-2. Power amplifier industry survey, devices available as of 2005.

item	part number	technology	dimensions	manufacturer	freq. band (MHz)	voltage (Volts)	DC power (mWatts)	P <sub>1dB</sub> (Watts)	gain (dB)
1	TGA9092	GaAs MESFET	0.25 um	Triquint	6000 - 18000	8.0	9600.0	2.818	24.0
2	FLL177ME	GaAs MESFET	TBD	Eudyna	500 - 1500	5.0	1500.0	1.995	11.5
3	RF2126	GaAs HBT	TBD	RF Micro Devices	1800 - 2500	6.0	2100.0	1.585	12.0
4	HMC414MS8G	GaAs InGaP HBT	proprietary	Hittite	2200 - 2800	5.0	1500.0	0.794	20.0
5	TGA8014	GaAs MESFET	TBD	Triquint	6000 - 18000	8.0	2728.0	0.794	11.0
6	HMC454ST89	GaAs InGaP HBT	proprietary	Hittite	400 - 2500	5.0	750.0	0.251	11.0
7	P0120002P	GaAs MESFET	TBD	Sumitomo Electric	0 - 2700	6.0	600.0	0.200	15.0
8	TGA2702	GaAs MESFET	TBD	Triquint	2300 - 2800	6.0	4500.0	0.158	28.0
9	RF2046	GaAs HBT	TBD	RF Micro Devices	0 - 3000	3.5	122.5	0.019	21.0

Table A-3. RF switches available from industry survey, devices available as of 2005

item	part number	technology	dimensions	manufacturer	freq. band (MHz)	voltage (Volts)	DC power (mWatts)	P <sub>IN_MAX</sub> (dBmW)	isolation (dB)
1	MASWSS0184	GaAs PHEMT	0.5 um	M/A - COM	0 - 4000	3.0	0.0	34.0	24.0
2	HMC484MS8G	GaAs	0.5 um	Hittite	0 - 3000	5.0	0.0	32.0	26.0
3	RSW-2-25P	GaAs	0.5 um	Mini-Circuits	0 - 2500	5.0	0.8	28.0	30.0
4	MASW-007588	GaAs PHEMT	0.5 um	M/A - COM	0 - 6000	3.0	75.0	28.0	21.0
5	SW90-0002	GaAs PHEMT	0.5 um	M/A - COM	0 - 4000	5.0	40.0	25.0	30.0
6	MASW-007587	GaAs PHEMT	0.5 um	M/A - COM	0 - 4000	3.0	0.0	25.0	24.0
7	HMC546LP2E	GaAs	0.5 um	Hittite	200 - 2700	3.0	0.0	38.0	10.0
8	SW-425	GaAs PHEMT	0.5 um	M/A - COM	0 - 3000	5.0	0.1	29.0	10.0
9	SW-283	GaAs	1.0 um	M/A - COM	0 - 3000	-5.0	0.1	27.0	20.0
10	MASWSS0180	GaAs PHEMT	1.0 um	M/A - COM	0 - 2500	-5.0	0.2	25.0	35.0
11	AS130-73	GaAs FET	TBD	Skyworks	0.3 - 2500	-5.0	1.0	24.0	18.0
12	A230-348	GaAs FET	TBD	Skyworks	0 - 6000	-10.0	6.0	30.0	13.0
13	MSP2TA-18	mechanical	TBD	Mini-Circuits	0 - 18000	24.0	5160.0	31.0	60.0
14	MTS-188	mechanical	TBD	Mini-Circuits	0 - 18000	24.0	5160.0	31.0	60.0

Table A-4. Phase modulators available from vendors as of 2005.

item	part number	technology	dimensions	manufacturer	freq. band (MHz)	voltage (Volts)	power (mWatts)	mod. BW (MHz)	P <sub>SB</sub> (dBmW)
1	TRF3702	SiGe	TBD	Texas Instruments	1500 - 2500	5.0	725.0	700.0	-37.0
2	HMC497LP4,E	SiGe	proprietary	Hittite	100 - 4000	5.0	840.0	700.0	-37.0
3	STQ-3016, Z	SiGe	1.0 um	Sirenza	2500 - 4000	5.0	400.0	500.0	-47.0
4	AD8349	SiGe	2.5 um	Analog Devices	700 - 2700	5.0	675.0	160.0	-34.6
5	IQBG-2000A	SiGe	TBD	Mini Circuits	1800 - 2000	—	—	10.0	-41.5
5	STQ-1016, Z	SiGe	1.0 um	Sirenza	250 - 1000	5.0	430.0	500.0	-46.0
6	STQ-2016, Z	SiGe	2.0 um	Sirenza	700 - 2500	5.0	430.0	500.0	-47.0
7	STQ-3016, Z	SiGe	3.0 um	Sirenza Microdevices	2500 - 4000	5.0	440.0	500.0	-44.0